Supporting Information for

Boosting the photocatalytic performance via isomeric configuration design in covalent organic frameworks

Fan Yang, *[#a] Hong-Yan Qu, [#a] Yuan Guo, [b] Jing-Lan Kan[a] and Yu-Bin Dong*[a]

[a]College of Chemistry, Chemical Engineering and Materials Science, Collaborative Innovation Center of Functionalized Probes for Chemical Imaging in Universities of Shandong, Key Laboratory of Molecular and Nano Probes, Ministry of Education, Shandong Normal University, Jinan 250014, P. R. China.
[b]School of Light Industry and Engineering, Qilu University of Technology (Shandong Academy of Sciences), Jinan 250353, China.

Contents

1. Materials and measurements (page S3)
2. Synthesis of the monomers and **COFs** (page S4-S9)
3. Simulated AB stacking models (page S9-S10)
4. Characterization of **COFs** (page S10-S12)
5. CV Curves (page S13)
6. Photocatalytic performance (page S13-S35)
7. Sunlight irradiation (page S35)
8. Photocurrent curves (page S36)
9. DFT calculations (page S36)
10. ESR spectrums (page S37)
11. Crystallographic parameters (page S37-S40)

1. Materials and measurements

The synthetic procedures were performed under argon atmosphere. Commercial chemicals (from sigma-Aldrich, JK Chemical and TCI) were used as received.

^{1}H-NMR and ^{13}C-NMR spectra of intermedia products, monomers and catalytic products were recorded at 400 MHz on a Bruker Avance spectrometer with tetramethylsilane (TMS) as the internal standard. Powder X-ray diffraction (PXRD) data were collected using a D8 ADVANCE X-ray with Cu Kα radiation (λ = 1.5405 Å). Fourier Transform Infrared (FT-IR) spectra in the region of 400-4000 cm^{-1} were obtained with a Perkin-Elmer 1600 FT-IR spectrometer. Ultraviolet–visible (UV−*vis*) absorption spectra were recorded on a Shimadzu UV-2600 Double Beam UV−vis Spectrophotometer. Cyclic voltammetry (CV) measurement was performed on a CHI660E electrochemical workstation in a three-electrode system. The working electrode was prepared by dropcasting an 5% Nafion (50 *u*L) suspension of COF (0.2 mg) and carbon black (0.7 mg) onto a glassy carbon electrode. The auxiliary electrode and reference electrode were platinum-wire and $Ag/AgNO_3$, and the electrolyte was 0.1 M tetrabutylammonium hexafluorophosphate in acetonitrile, Ferrocene was used as a standard to calculate the energy levels vs. vacuum. Thermogravimetric analysis (TGA) was performed on a TGA/DSC 3+ in the temperature range of 30-800 ºC under a nitrogen atmosphere and a heating rate of 10 °C/min. Scanning electron microscopy (SEM) images were performed on a SUB010 scanning electron microscope with acceleration voltage of 20 kV. Solid state ^{13}C CP-MAS spectrum was acquired at BRUKER AVANCE NEO 400WB. N_2 adsorption-desorption isotherm was obtained using an ASAP 2020/TriStar 3000 (Micromeritics) apparatus measured at 77 K, the sample was degassed at 100 ºC for 12 h under high vacuum before analysis. High resolution mass spectrometry (HRMS) analysis was detected by Bruker maXis ultrahigh-resolution-TOF mass spectrometer. The models of LED lamp is PL-SX100A. Electron paramagnetic resonance (EPR) spectra was measured by Bruker A300 EPR Spectroscopy. The electrochemical impedance spectra (EIS) was performed by Correst Electrochemical Workstation CS310H. Chenhua electrochemical workstation (CHI660D Instruments, Shanghai Chenhua Instrument Co., Ltd., Shanghai, China) was used to measure the photocurrent. Transmission electron microscopy (TEM) images and corresponding elemental mapping images was measured by FEI Talos F200X American FEI.

2. Synthesis of the monomers and COFs

2.1 Synthesis of the monomers

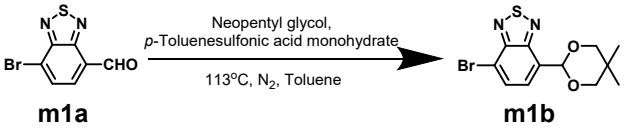

Scheme S1 Synthesis procedure of 4-bromo-7-(5,5-dimethyl-1,3-dioxan-2-yl)benzo[*c*][1,2,5]thia diazole (**m1b**)

Synthesis of m1b. To a 100 mL pressure tube was added 7-bromo-benzo[*c*][1,2,5]thiadiazole-4-carbaldehyde (m1a, 1.5 g, 6.17 mmol), Neopentyl glycol (778.6 mg, 7.48 mmol), *p*-Toluenesulfonic acid monohydrate (35.2 mg, 0.19 mmol) and 10 mL Toluene. Then the reaction system was degassed-inflated with nitrogen three times. After stirring overnight at a temperature of 113 ℃, the system was cooled to room temperature. The liquid was extracted three times with saturated $NaHCO_3$ solution and ethyl acetate and the organic phase was collected. The organic phase was dried over anhydrous $MgSO_4$ and the solvent was removed in vacuo. The crude product was purified by silica gel chromatography (dichloromethane: petroleum ether, v/v = 2:1 as eluent) to obtain **m1b** as a white powder (1.96 g, 97% of yield). ^{1}H-NMR ($CDCl_3$, 400 MHz): δ(ppm) 7.89-7.87 (d, *J* = 8.0 Hz, 1H), 7.80-7.78 (d, *J* = 8.0Hz, 1H), 6.12 (s, 1H), 3.86-3.79 (m, *J* = 28.0 Hz, 4H), 1.35 (s, 3H), 0.85 (s, 3H). ^{13}C-NMR ($CDCl_3$, 100 MHz): δ(ppm) 153.43, 152.39, 131.89, 130.45, 127.35, 114.86, 97.79, 77.93, 30.46, 23.04, 21.85. HR-MS (EI): m/z $[M+H]^+$ calcd for $C_{12}H_{12}BrN_2O_2S$: 328.9959, found: 328.9919.

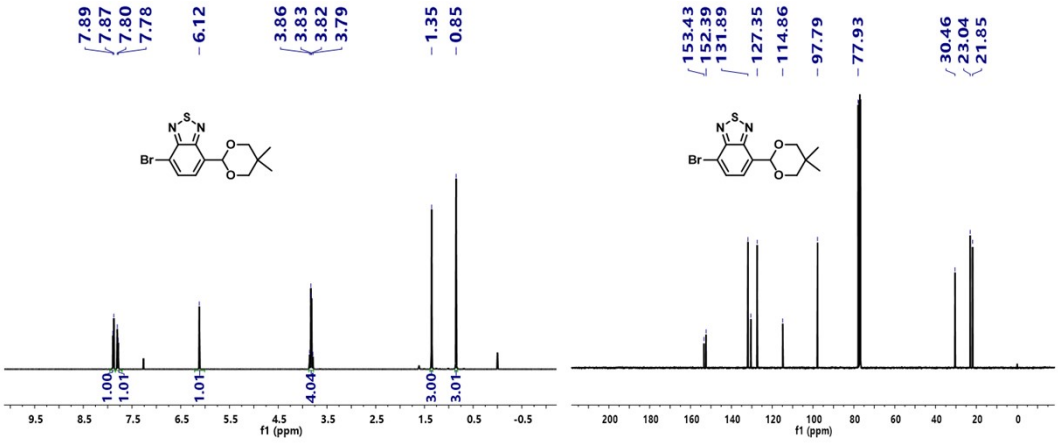

Fig. S1 The ^{1}H-NMR (left) and ^{13}C-NMR spectrums of **m1b**.

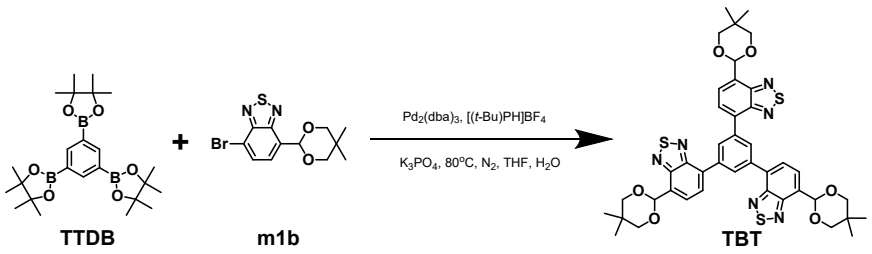

Scheme S2 Synthesis procedure of **TBT**.

Synthesis of TBT. To a 100 mL pressure tube was added 1,3,5-tris(4,4,5,5-tetramethyl-1,3,2-dioxaborolan-2-yl)benzene (TTDB, 730.5 mg, 1.60 mmol), 4-bromo-7-(5,5-dimethyl-1,3-dioxan-2-yl)benzo[*c*][1,2,5]thiadiazole (m1b, 1.74 g, 5.29 mmol), [(*t*-Bu)PH]BF_4 (32.5 mg, 0.11 mmol), 1 mL K_3PO_4 aqueous solution (2M) and 10 mL THF. Then the mixture was degassed-inflated with nitrogen three times before $Pd_2(dba)_3$ (29.3 mg, 0.03 mmol) was added. The reaction system was heated up to 80 ℃ for 24 h. After the reaction system was cooled to room temperature, the reaction solution was extracted three times with ethyl acetate and saturated NaCl solution and then the organic phase was collected. After drying over anhydrous $MgSO_4$, the solvent was removed in vacuo. The crude product was purified by silica gel chromatography (dichloromethane:ethyl acetate, v/v = 50:1 as eluent) to obtain **TBT** as light yellow powder (950 mg, 73% of yield). ^{1}H-NMR ($CDCl_3$, 400 MHz): δ(ppm) 8.52 (s, 3H), 8.08-8.07 (d, *J* = 4.0 Hz, 3H), 7.95-7.93 (d, *J* = 8.0 Hz, 3H), 6.26 (s, 3H), 3.90-3.84 (m, *J* = 24.0 Hz, 12H), 1.39 (s, 9H), 0.87 (s, 9H). ^{13}C-NMR ($CDCl_3$, 100 MHz): δ(ppm) 153.68, 153.36, 137.95, 134.50, 130.43, 130.16, 128.16, 127.00, 98.16, 77.98, 30.52, 23.09, 21.92.HR-MS (EI): m/z $[M+Na]^+$ calcd for $C_{42}H_{42}N_6O_6S_3$ 845.2226, found: 845.2264.

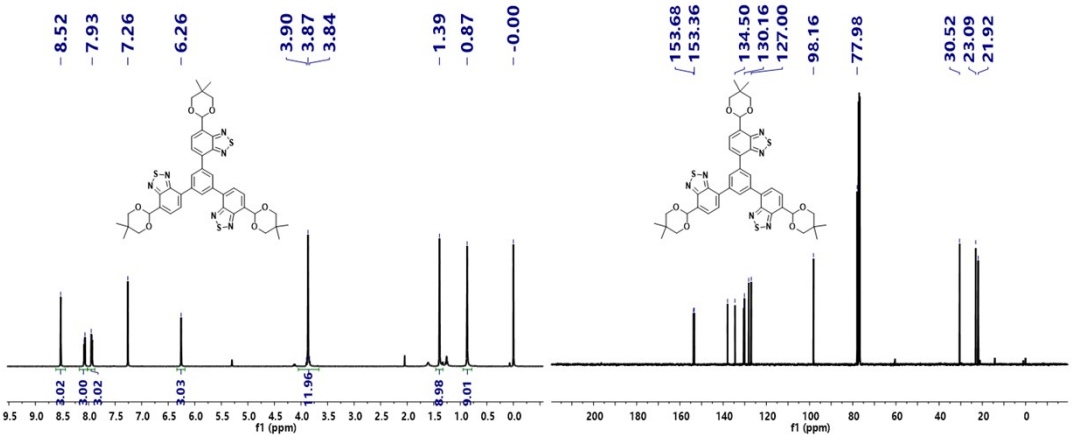

Fig. S2 The ^{1}H-NMR (left) and ^{13}C-NMR spectrums of **TBT**.

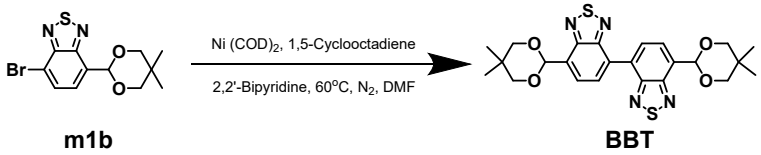

Scheme S3 Synthesis procedure of **BBT**

Synthesis of BBT. $Ni(COD)_2$ (601.57 mg, 2.19 mmol), 1,5-cyclooctadiene (197.2 mg, 1.82 mmol), and bipyridine (341.6 mg, 2.19 mmol) were dissolved in 10 mL of dry DMF in a Schlenk tube under N_2 atmosphere. Then the 4-bromo-7-(5,5-dimethyl-1,3-dioxan-2-yl)benzo[*c*][1,2,5]thiadiazole (m1b, 600 mg, 1.82 mmol) was added to the solution at room temperature. The reaction system was stirred at 60 ℃ overnight. After the reaction mixture was cooled to room temperature, the reaction solution was diluted with dichloromethane, and the filtrate was collected after suction filtration. The filtrate was extracted three times with 10% $FeCl_3$ solution, and the organic phase was collected. The organic phase was dried over anhydrous $MgSO_4$ and the solvent was removed in vacuo. The crude product was purified by silica gel chromatography (dichloromethane as eluent) to obtain **BBT** as bright yellow powder (200 mg, 44% of yield). ^{1}H-NMR ($CDCl_3$, 400 MHz): δ(ppm) 8.27-8.25 (d, J = 8.0 Hz, 2H), 8.11-8.09 (d, J = 8.0 Hz, 2H), 6.26 (s, 2H), 3.90-3.84 (m, J = 24.0 Hz, 6H), 1.39 (s, 3H), 0.87 (s, 3H). ^{13}C-NMR ($CDCl_3$, 100 MHz): δ(ppm) 153.79, 153.23, 130.82, 130.39, 126.72, 77.97, 98.09, 30.51, 23.07, 21.91. HR-MS (EI): m/z $[M+H]^+$ calcd for $C_{24}H_{26}N_4O_4S_2$ 499.1468, found: 499.1455.

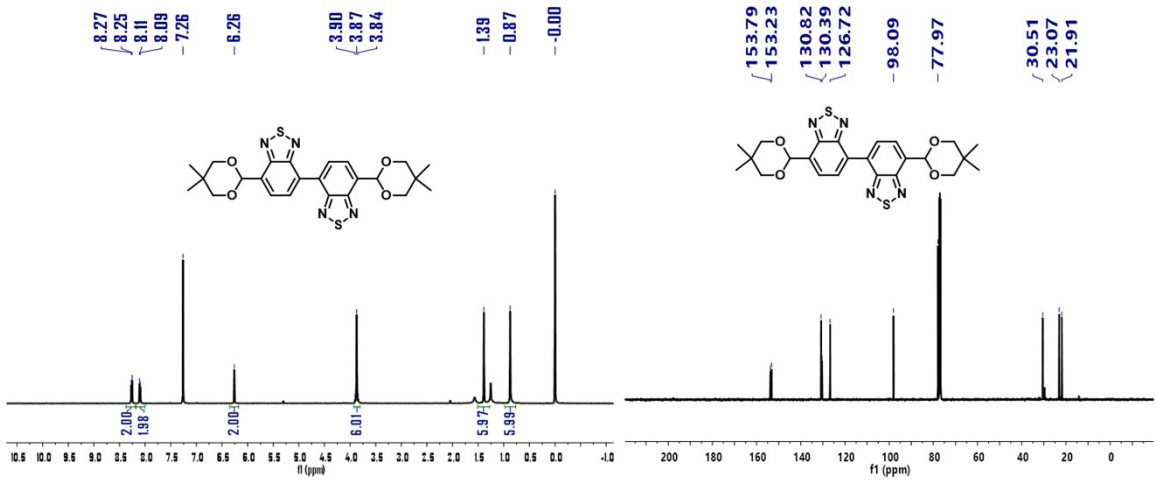

Fig. S3 The ^{1}H-NMR (left) and ^{13}C-NMR spectrums of **BBT**.

2.2 Model Reaction

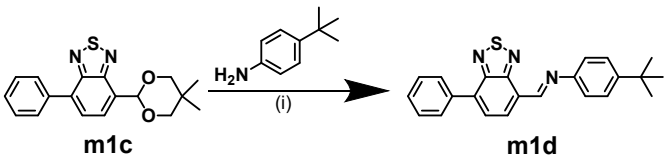

Scheme S4 The synthetic procedure of condensation reaction. i: o-dichlorobenzene/n-bytanol/acetic acid (6 M) and trifluoroacetic acid (0.6 M) (1 /1/0.2 mL, v/v/v), 120 °C, 24h.

m1c: m1c was prepared via Suzuki-Miyaura coupling reaction between m1b and phenylboronic acid with 81% of yield. ^{1}H-NMR ($CDCl_3$, 400 MHz): δ(ppm) 8.02-8.00 (d, *J* = 8.0 Hz, 1H), 7.90-7.88 (d, *J* = 8.0 Hz, 2H), 7.74-7.73 (d, *J* = 4.0 Hz, 1H), 7.54-7.51 (t, *J* = 12.0 Hz, 2H), 7.46-7.43 (t, *J* = 12.0 Hz, 1H), 6.23 (s,1H), 3.89-3.83 (m, *J* = 24.0 Hz, 4H), 1.39 (s, 3H), 0.86 (s, 3H). ^{13}C-NMR ($CDCl_3$, 100 MHz): δ (ppm) 153.66, 153.33, 137.31, 135.08, 128.63, 128.53, 127.73, 126.94, 98.20, 78.00, 30.52, 23.10, 21.92. HR-MS (EI): m/z $[M+Na]^+$ calcd for $C_{18}H_{18}N_2O_2S$ 349.0987, found: 349.1096.

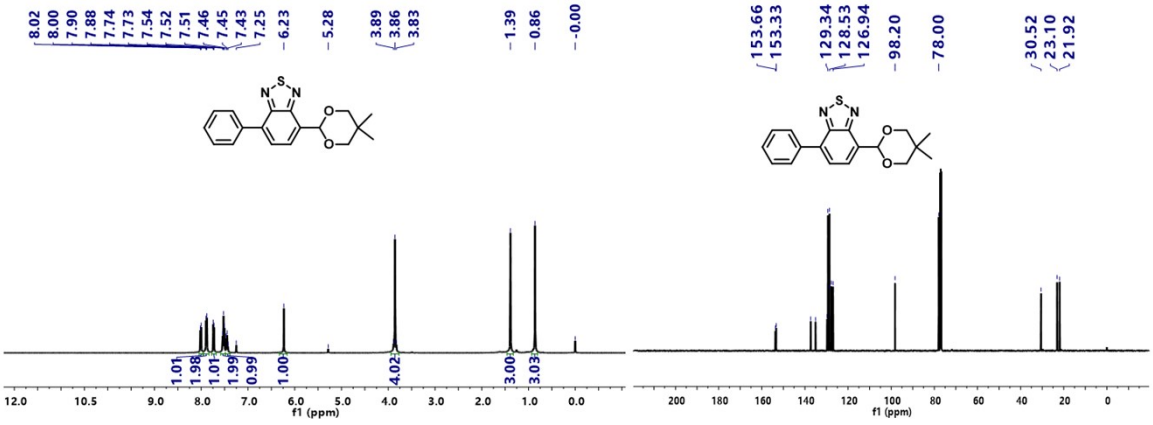

Fig. S4 The ^{1}H-NMR (left) and ^{13}C-NMR spectrums of **m1c**.

m1d: m1c (150 mg,0.46 mmol), tert-butylaniline (102.87 mg,0.69 mmol), 2 ml o-dichlorobenzene, 2 ml n-butanol and 400 μl of mixed aqueous solution of trifluoroacetic acid(0.6 M) and acetic acid(6 M) were added to a 100 ml pressure-resistant tube, and nitrogen was evacuated three times. The reaction system was heated to 120 ℃ and held for 24 hours. After the reaction, the system was cooled to room temperature, extracted three times with dichloromethane and saturated brine. The organic phase was collected and the solvent was removed in vacuo. The obtained crude product was purified by silica gel chromatography with petroleum ether:ethyl

acetate=15 : 1 to obtain bright yellow solid **m1d** (158.4 mg, 93% yield). ^{1}H-NMR ($CDCl_3$, 400 MHz): δ (ppm) 9.43 (s, 1H), 8.54-8.52 (d, *J* = 8.0 Hz, 1H), 8.00-7.98 (m, *J* = 8.0 Hz, 2H), 7.87-7.86 (d, *J* = 4.0 Hz, 1H), 7.59-7.55 (t, *J* = 16.0 Hz, 2H), 7.51-7.46 (m, *J* = 20.0 Hz, 3H), 7.36-7.34 (d, *J* = 8.0 Hz, 2H), 1.37 (s, 9H). ^{13}C-NMR ($CDCl_3$, 100 MHz): δ (ppm) 154.88, 153.72, 149.95, 149.06, 136.62, 129.60, 129.40, 128.90, 128.72, 127.93, 127.43, 126.16, 121.02, 34.63, 31.45. HR-MS (EI): m/z $[M+H]^+$ calcd for $C_{23}H_{21}N_3S$ 372.1536, found: 372.1491.

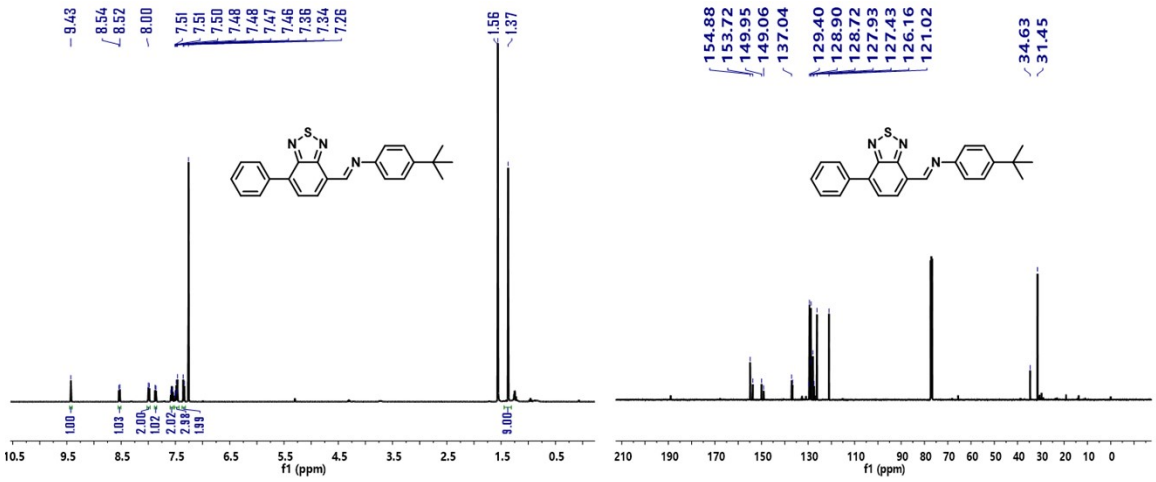

Fig. S5 The ^{1}H-NMR (left) and ^{13}C-NMR spectrums of m1d.

2.3 Synthesis of COFs

2.3.1 Synthesis of BT-COF1

To a 10 mL Pyrex tube was added 1,3,5-tris(7-(5,5-dimethyl-1,3-dioxan-2-yl)benzo[*c*][1,2,5]thiadiazol-4-yl)benzene (TBT, 30 mg, 0.036 mmol), 4,4'-diaminobiphenyl (DABP, 10 mg, 0.054 mmol) and o-dichlorobenzene/n-Butanol (1:1 v/v, 2 mL). After the mixture was sonicated for 1 min, 0.2 mL of mixed aqueous solution of trifluoroacetic acid (0.6 M) and acetic acid (6 M) were added. After the mixture was sonicated for another 20s again, the tube was flash frozen at 77 K using a liquid N_2 bath and degassed by three freeze-pump-thaw cycles, sealed under vacuum and then heated at 120 ℃ for 3 days. A red precipitate was formed, which was collected by sucking filtration and throughly washed with acetone, anhydrous ethanol, tetrahydrofuran, and dichloromethane, respectively. The collected sample was dried under vacuum at 120 ℃ for 24 h to give a red powder (26 mg, 92 % of yield).

2.3.2 Synthesis of BT-COF2

To a 10 mL Pyrex tube was added 7-(5,5-dimethyl-1,3-dioxan-2-yl)-7'-(2,2-dimethyl-1,3-dioxan-5-yl)-4,4'-bibenzo[c][1,2,5]thiadiazole (BBT, 15 mg, 0.03 mmol), 5'-(4-aminophenyl)-[1,1':3',1"-terphenyl]-4,4"-diamine (TAPB, 7 mg, 0.02 mmol) and o-dichlorobenzene/n-Butanol (1:1 v/v, 1 mL). After the mixture was sonicated for 1 min, 0.1 mL of mixed aqueous solution of trifluoroacetic acid (0.6 M) and acetic acid (6 M) were added. After the mixture was sonicated for another 20 s again, the tube was flash frozen at 77 K using a liquid N_2 bath and degassed by three freeze-pump-thaw cycles, sealed under vacuum and then heated at 120 ℃ for 3 days. A black precipitate was formed, which was collected by sucking filtration and thoroughly washed with acetone, anhydrous ethanol, tetrahydrofuran, and dichloromethane, respectively. The collected sample was dried under vacuum at 120 ℃ for 24 h to give a dark powder (15 mg, 91% of yield).

3. Simulated AB stacking models

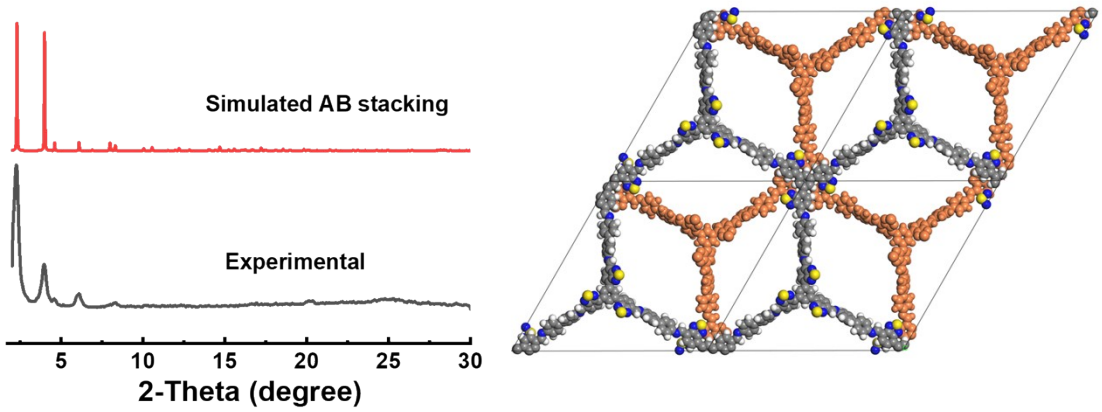

Fig. S6 Comparison of the experimental (black) and simulated (red) AB stacking PXRD patterns of **BT-COF1** and the top view of the simulated structure of AB stacking method.

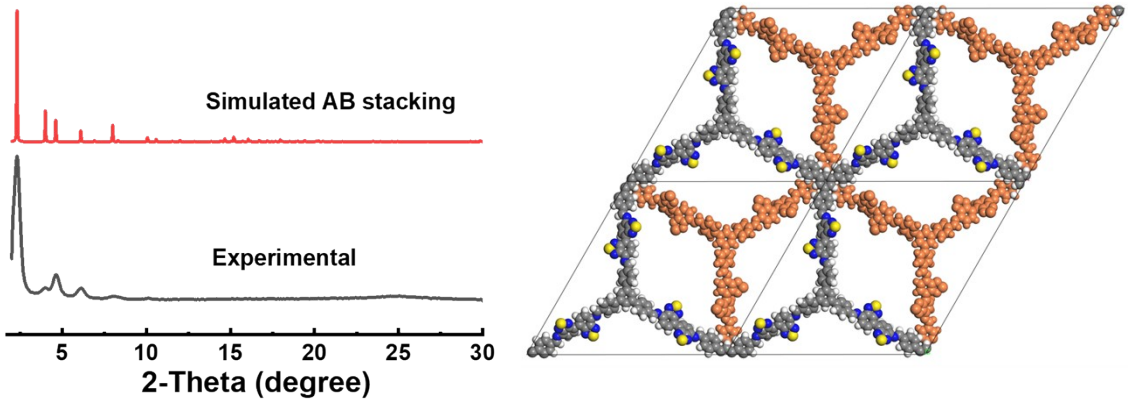

Fig. S7 Comparison of the experimental (black) and simulated (red) AB stacking PXRD patterns of **BT-COF2** and the top view of the simulated structure of AB stacking method.

4. Characterization of COFs

4.1. BET and pore size

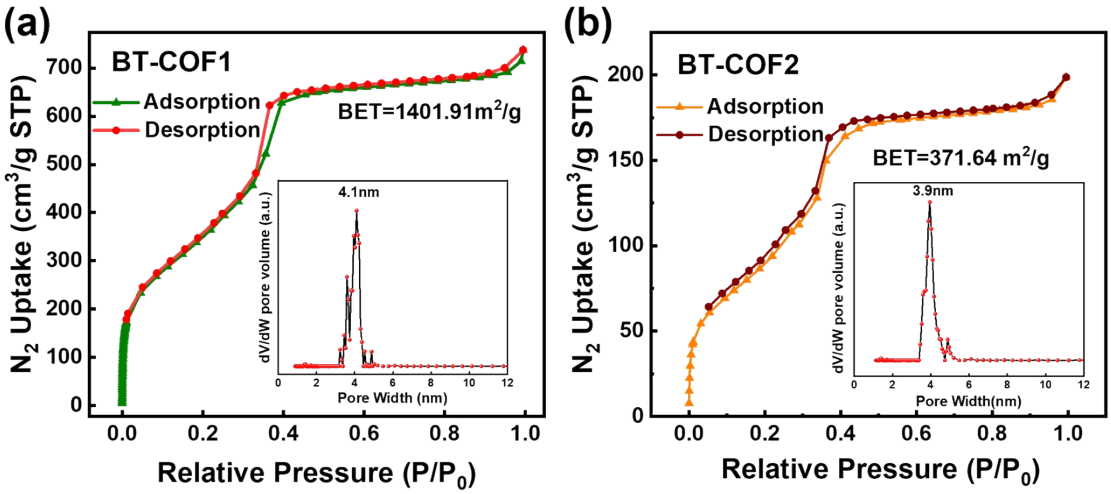

Fig. S8 The N_2 adsorption-desorption isotherms and pore size distribution profiles.

4.2. The FT-IR spectrum

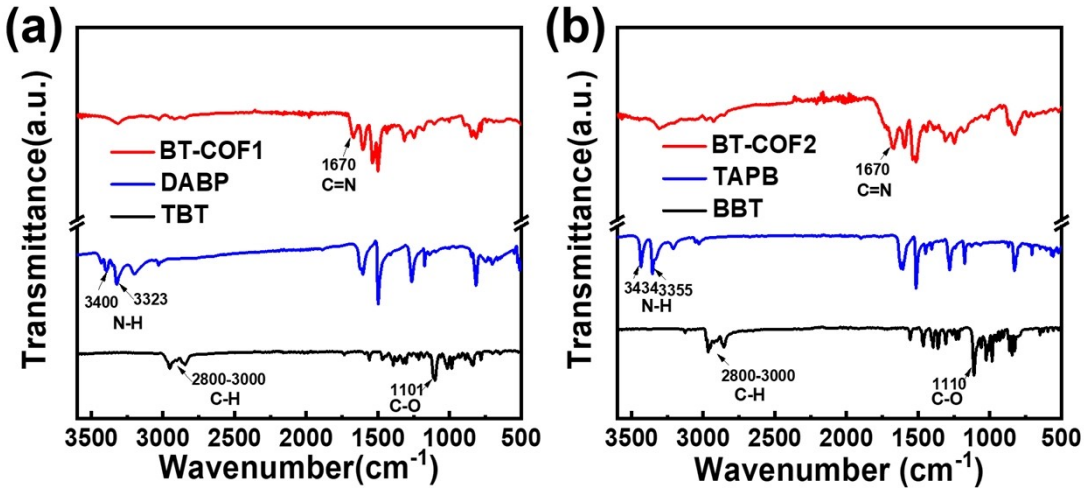

Fig. S9 The FT-IR spectra of the COFs.

4.3. Solid state ^{13}C CP/MAS NMR spectrum

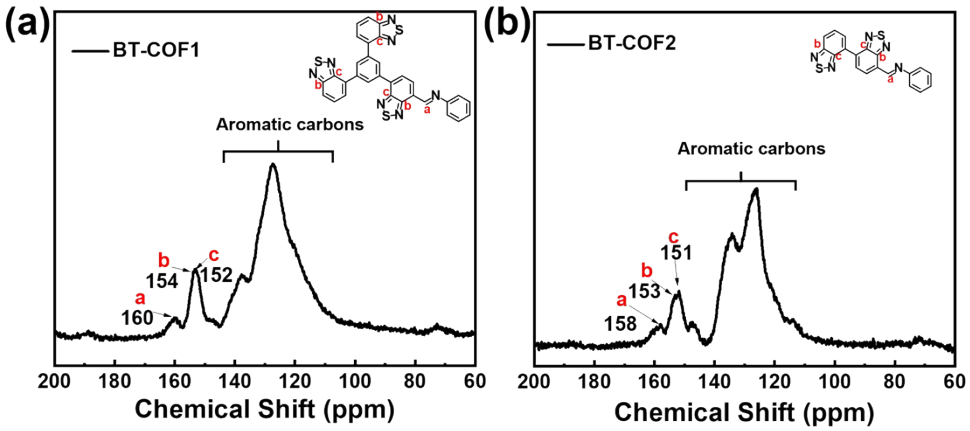

Fig. S10 The solid state ^{13}C CP/MAS NMR spectrums of the COFs.

4.4. SEM and TEM images

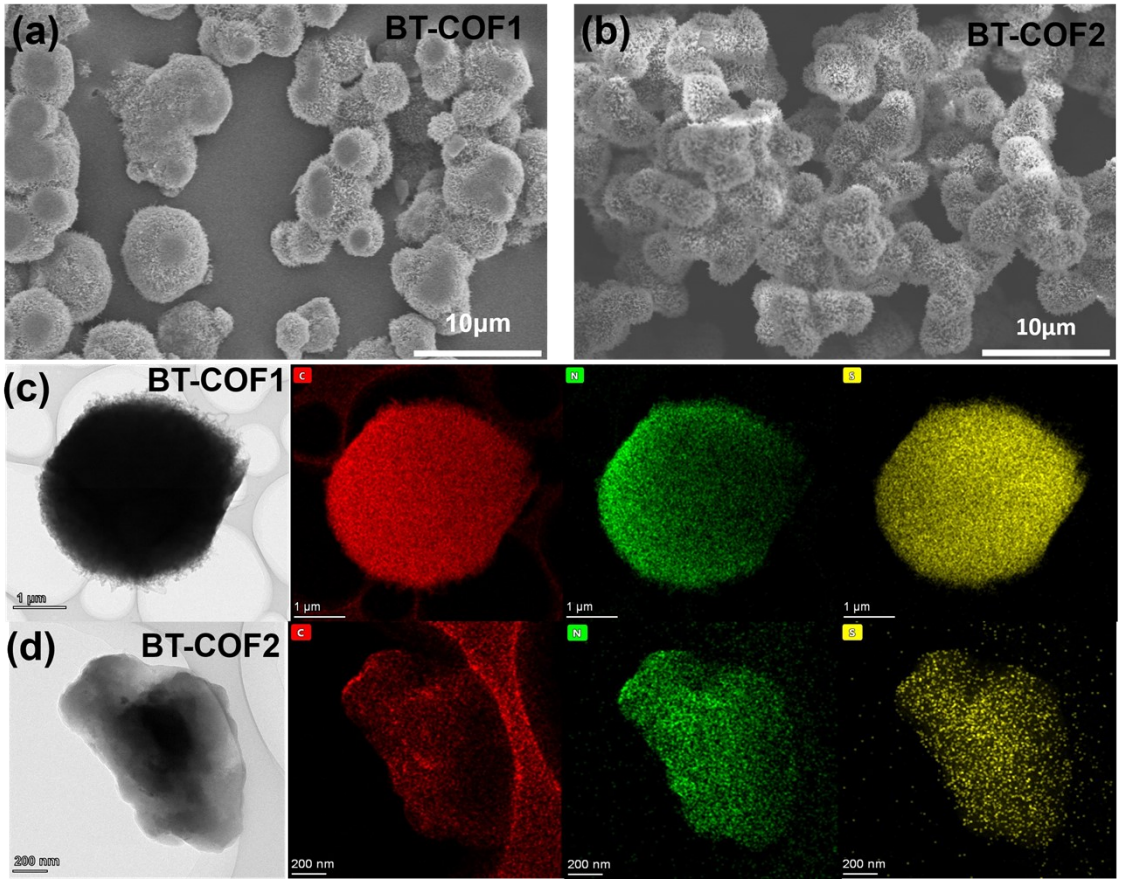

Fig. S11 Scanning electron microscopy (SEM) images of (a) **BT-COF1** and (b) **BT-COF2**. Transmission electron microscopy (TEM) images and corresponding elemental mapping images of (c) **BT-COF1** and (d) **BT-COF2**.

4.5. TGA curves

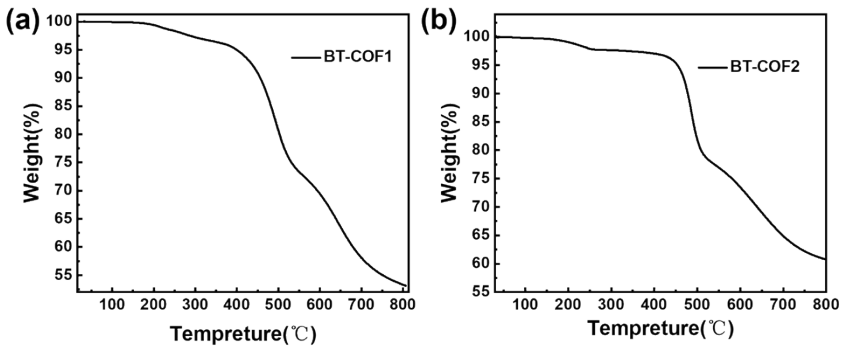

Fig. S12 TGA curve of (a) **BT-COF1** and (b) **BT-COF2.**

5. CV curves

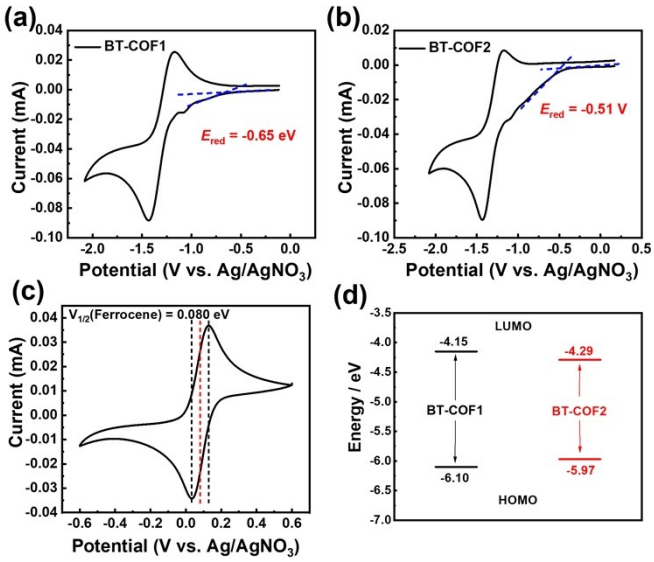

Fig. S13 Cyclic voltammetry graphs of (a) **BT-COF1**, (b) **BT-COF2**, (c) ferrocene and (d) energy levels.

The energy level of the COFs vs. vacuum were derived from the following equations.

$$E_{LUMO} = -(E_{red}(onset) - E_{1/2}(Fc) + 4.8)\ eV$$

$$E_{HOMO} = E_{LUMO} - E_g$$

6. Photocatalytic performance

6.1. General procedure for photooxidation reaction

A 10 mL quartz tube was charged with reaction substrate (0.3 mmol), COF (10 mg) and solvent (3 mL). The mixture was bubbled with oxygen and stirred, then the tube was irradiated with a 10 w blue LED lamp or natural sunlight in room temperature. After reaction, the solution was centrifuged and the supernatant was removed by rotary evaporation. Yields were determined by ^{1}H-NMR spectroscopy with 0.3 mmol diphenylacetonitrile (DPAT) as internal standard. The isolated yields was obtained by purifying the solution by silica gel flash chromatography (Petroleum ether and Ethyl acetate).

6.2. Yield of 2a determined by ^{1}H-NMR analysis

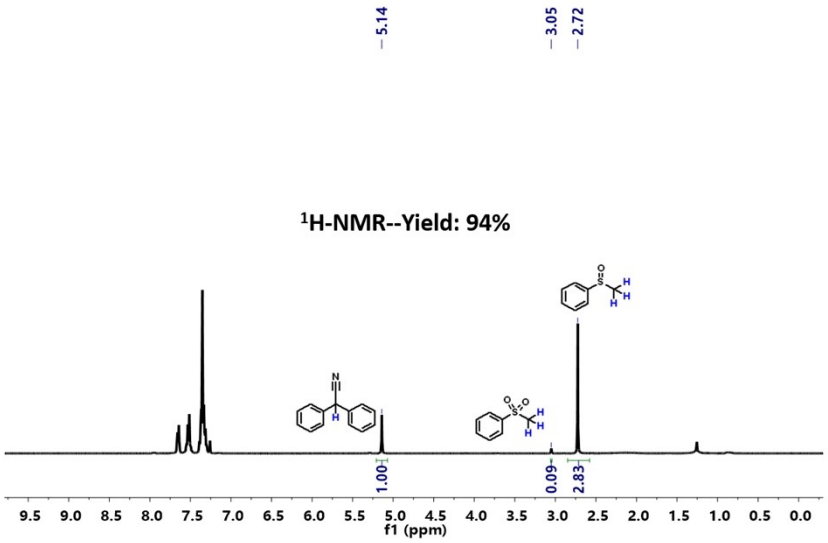

Fig. S14 Yield of **2a** catalyzed by **BT-COF2** and determined by ^{1}H-NMR with DPAT as internal standard.

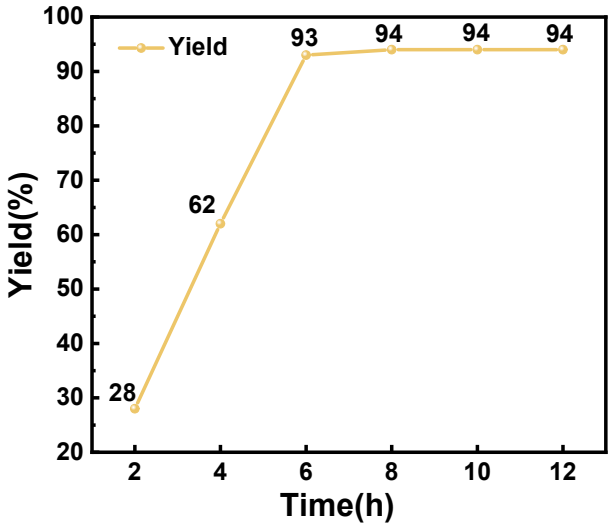

Fig. S15 Reaction time examination of **2a** based on **BT-COF2** as catalyst.

Isolated 2a: ^{1}H-NMR ($CDCl_3$, 400 MHz): δ (ppm) 7.68-7.65 (m, J = 12.0 Hz, 2H), 7.54-7.52 (m, J = 8.0 Hz, 3H), 2.74 (s, 3H). ^{13}C NMR ($CDCl_3$, 100 MHz): δ (ppm) 145.71, 131.04, 129.36, 123.49, 43.97. HR-MS (EI): m/z $[M+Na]^+$ calcd for C_7H_8OS 163.0194 found:163.0186.

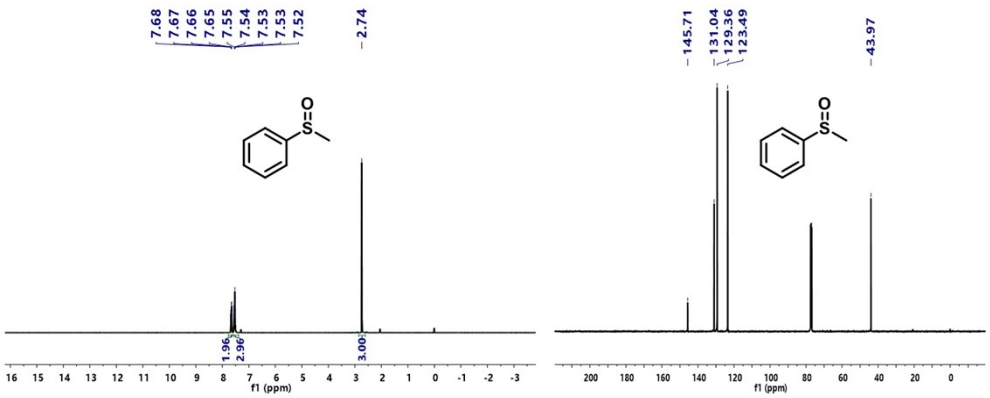

Fig. S16 ^{1}H-NMR (left) and ^{13}C-NMR (right) spectra of **2a**.

6.3. Control experiments

Table S1. The control experiment determined by ^{1}H-NMR analysis and isolated yield.

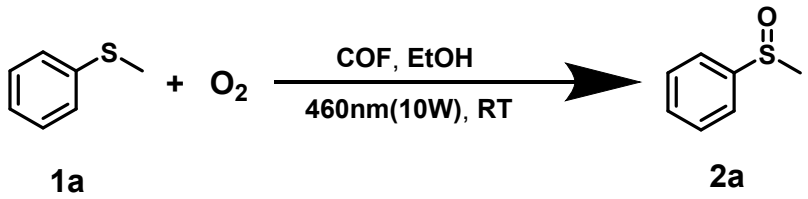

1a **2a**

Entry	Solvent	Light	Catalyst	O_2	Time (h)	Yield (%)
1	CH_3CN	460nm	BT-COF2	√	8	57[a] (53[b])
2	Toluene	460nm	BT-COF2	√	8	18 (11)
3	$CHCl_3$	460nm	BT-COF2	√	8	78 (72)
4	EtOH	460nm	BT-COF2	√	8	**94 (91)**
5	EtOH	460nm	-	√	8	0[a]
6	EtOH	460nm	BT-COF2	-	8	0[a]
7	EtOH	-	BT-COF2	√	8	<1[a]

[a] Yields determined by ^{1}H-NMR analysis. [b] Isolated yields.

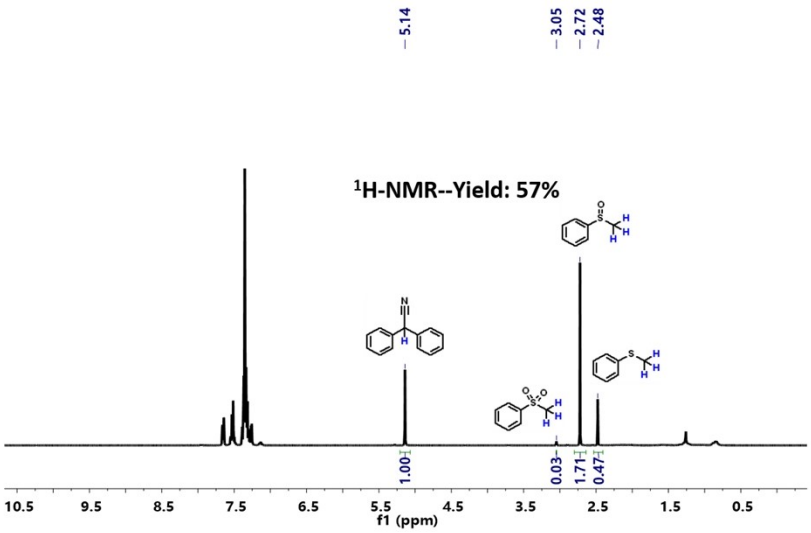

Fig. S17 Yield of **entry 1** determined by ^{1}H-NMR with DPAT as internal standard.

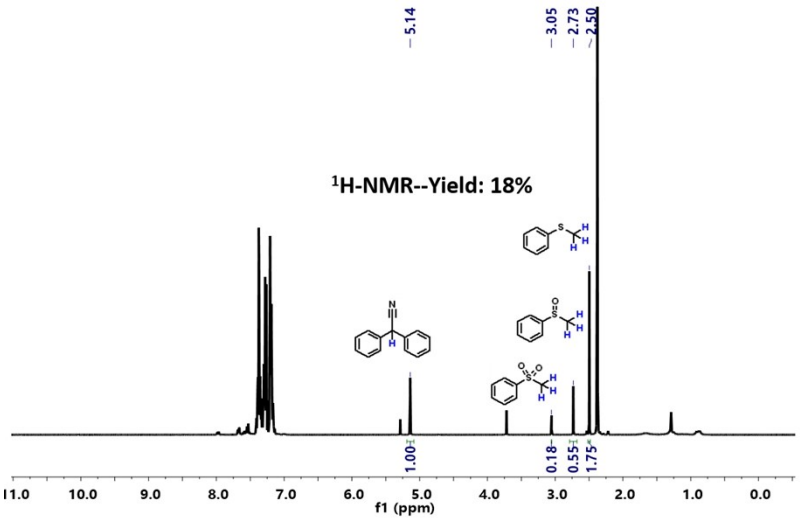

Fig. S18 Yield of **entry 2** determined by ^{1}H-NMR with DPAT as internal standard.

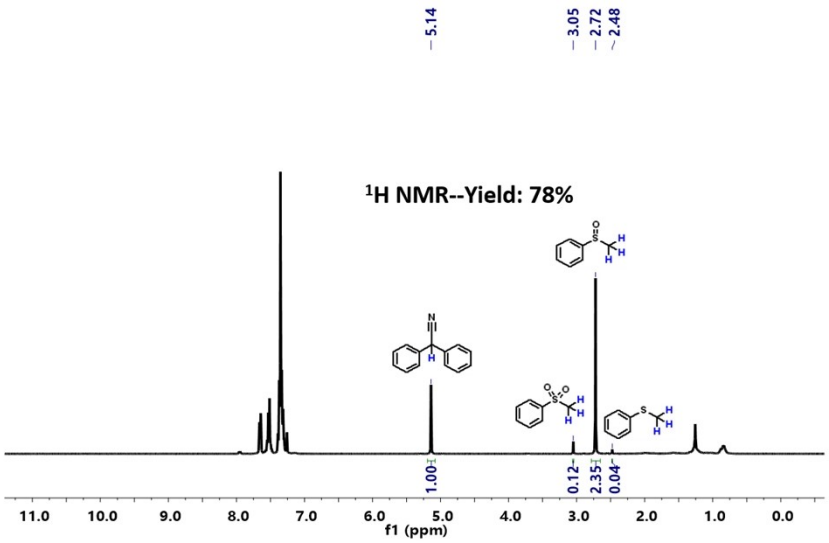

Fig. S19 Yield of **entry 3** determined by ^{1}H-NMR with DPAT as internal standard.

Fig. S20 Yield of **entry 4** determined by ^{1}H-NMR with DPAT as internal standard.

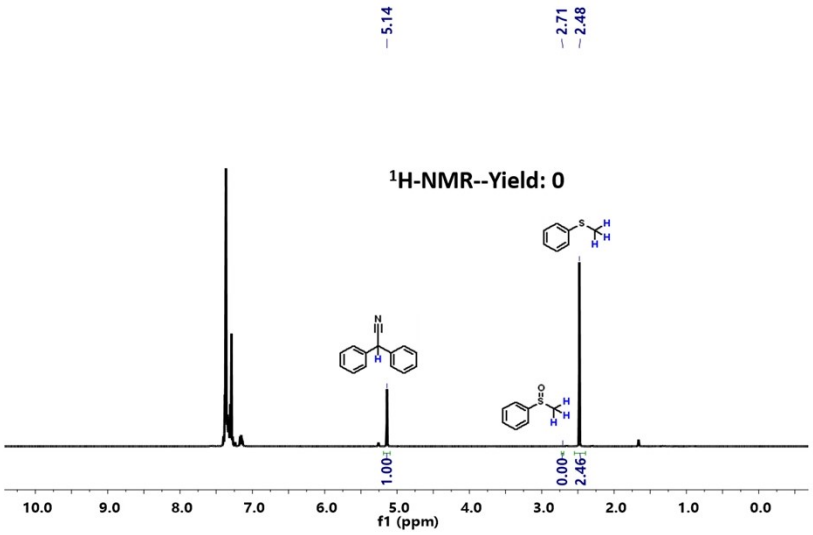

Fig. S21 Yield of **entry 5** determined by ^{1}H-NMR with DPAT as internal standard.

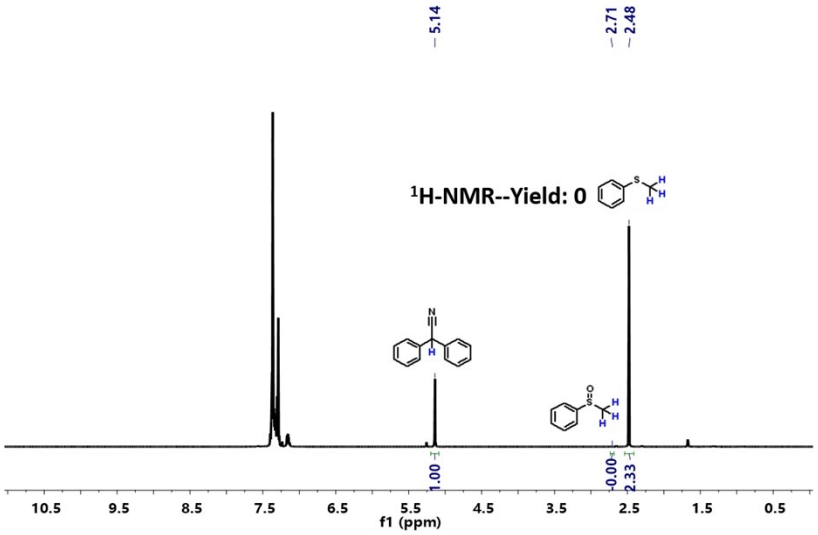

Fig. S22 Yield of **entry 6** determined by ^{1}H-NMR with DPAT as internal standard.

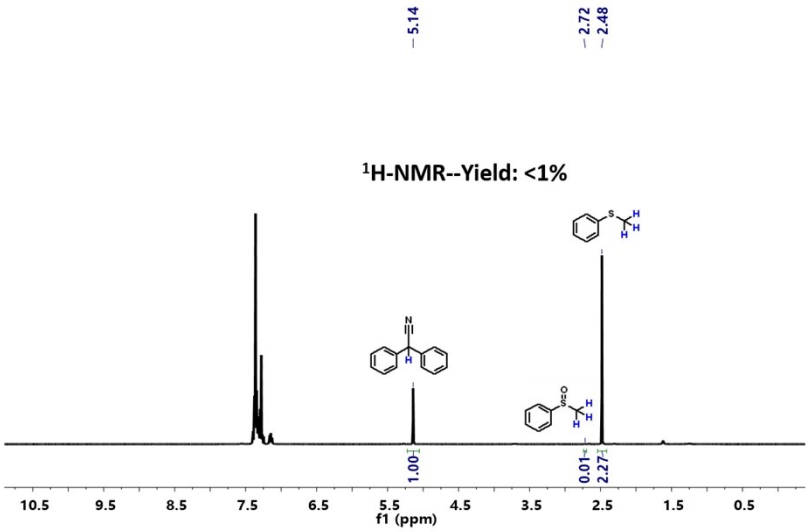

Fig. S23 Yield of **entry 7** determined by ^{1}H-NMR with DPAT as internal standard.

6.4. Comparison of the catalytic activities of two catalysts

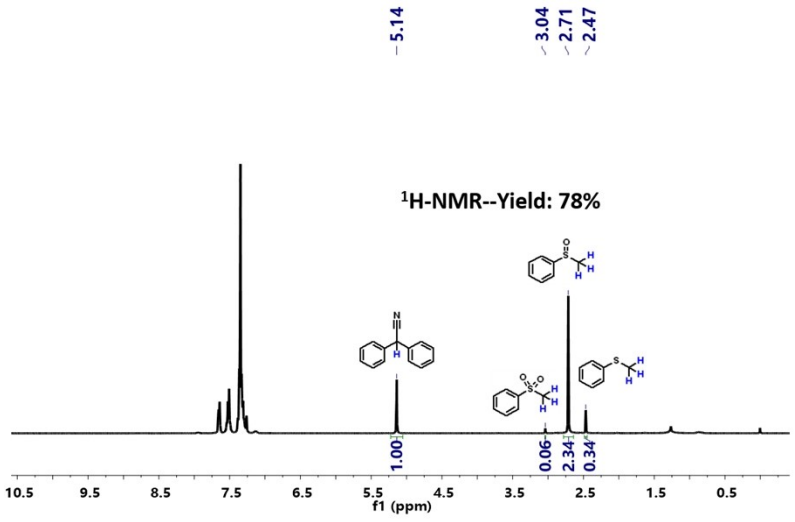

Fig. S24 Yield of 2**a** catalyzed by **BT-COF1** and determined by ^{1}H-NMR with DPAT as internal standard.

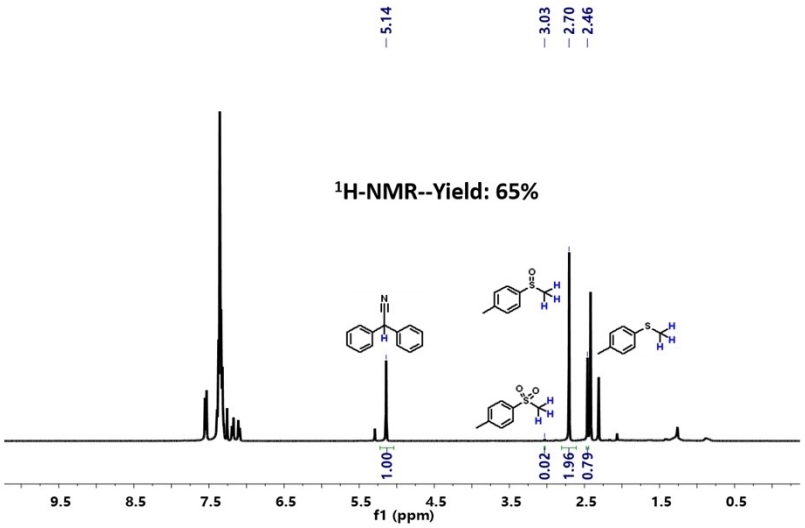

Fig. S25 Yield of 2**b** catalyzed by **BT-COF1** and determined by ^{1}H-NMR with DPAT as internal standard.

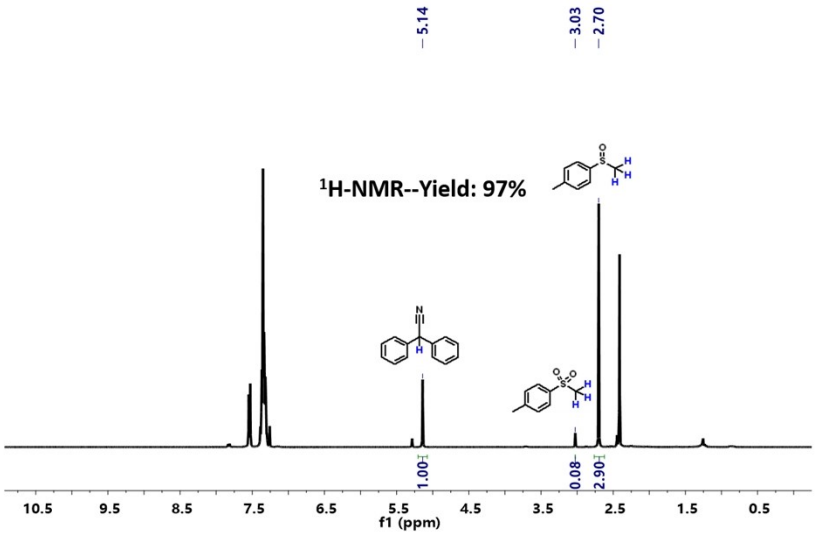

Fig. S26 Yield of 2**b** catalyzed by **BT-COF1** and determined by ^{1}H-NMR with DPAT as internal standard.

Isolated 2b: ^{1}H-NMR ($CDCl_3$, 400 MHz): δ (ppm) 7.55-7.53 (d, J = 8.0 Hz, 2H), 7.34-7.32 (d, J = 8.0 Hz, 2H), 2.70 (s, 3H), 2.41 (s, 3H). ^{13}C-NMR ($CDCl_3$, 100 MHz): δ (ppm) 142.44, 141.51, 130.02, 123.54, 43.92, 21.36. HR-MS (EI): m/z $[M+Na]^+$ calcd for $C_8H_{10}OS$ 177.0350, found: 177.0366.

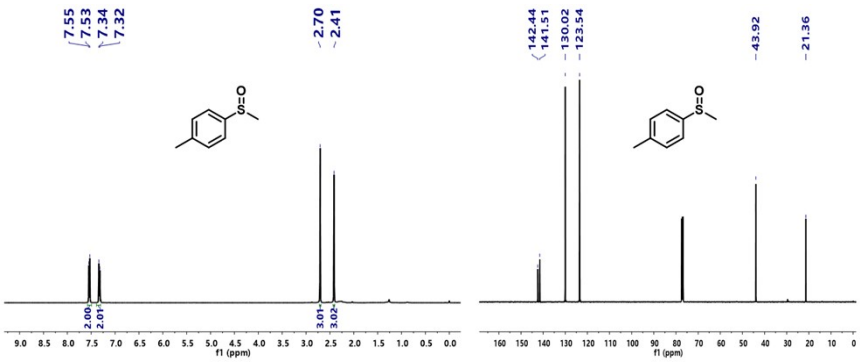

Fig. S27 ^{1}H-NMR (left) and ^{13}C-NMR (right) spectra of **2b**.

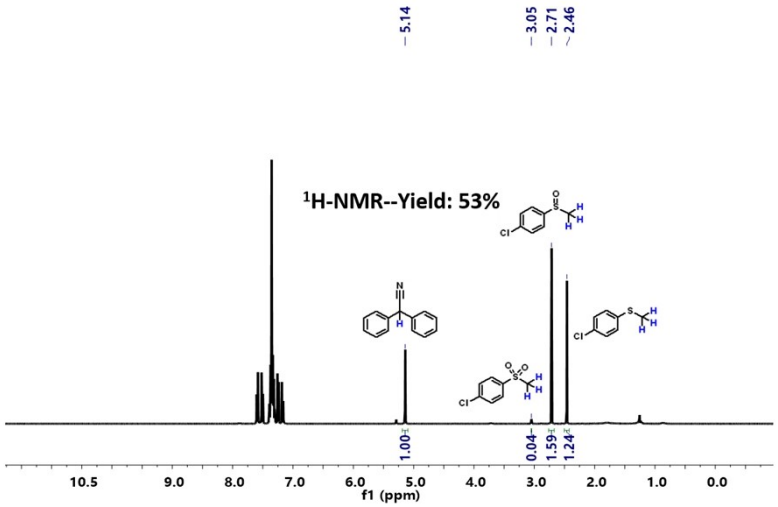

Fig. S28 Yield of **2c** catalyzed by **BT-COF1** and determined by ^{1}H-NMR with DPAT as internal standard.

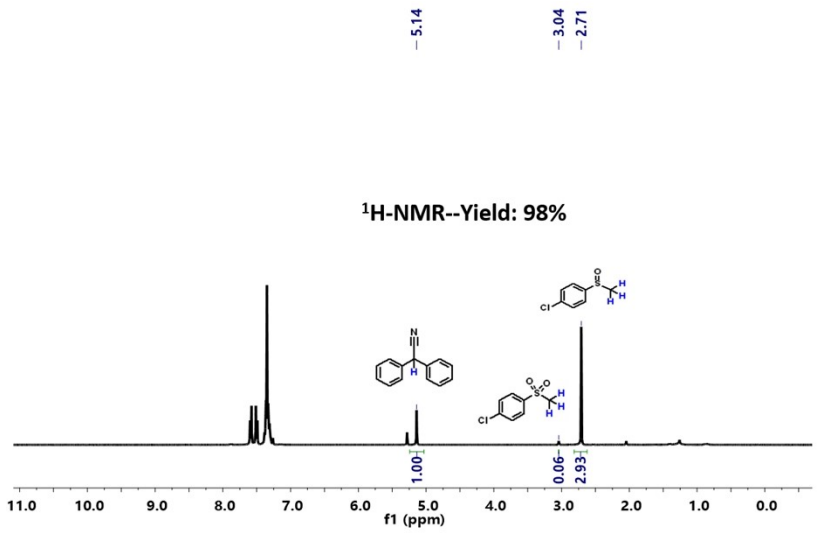

Fig. S29 Yield of **2c** catalyzed by **BT-COF2** and determined by ^{1}H-NMR with DPAT as internal standard.

Isolated 2c: ^{1}H-NMR ($CDCl_3$, 400 MHz): δ (ppm) 7.61-7.59 (d, J = 8.0 Hz, 2H), 7.52-7.50 (d, J = 8.0 Hz, 2H), 2.72 (s, 3H). ^{13}C-NMR ($CDCl_3$, 100 MHz): δ (ppm) 144.29, 137.23, 129.64, 124.98, 44.05. HRMS (ESI) m/z $[M+Na]^+$ calcd for C_7H_8ClOS:196.9804 found:196.9815.

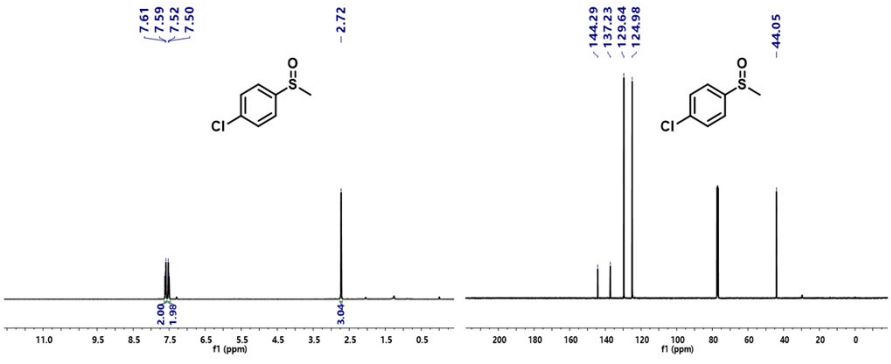

Fig. S30 ^{1}H-NMR (left) and ^{13}C-NMR (right) spectra of **2c.**

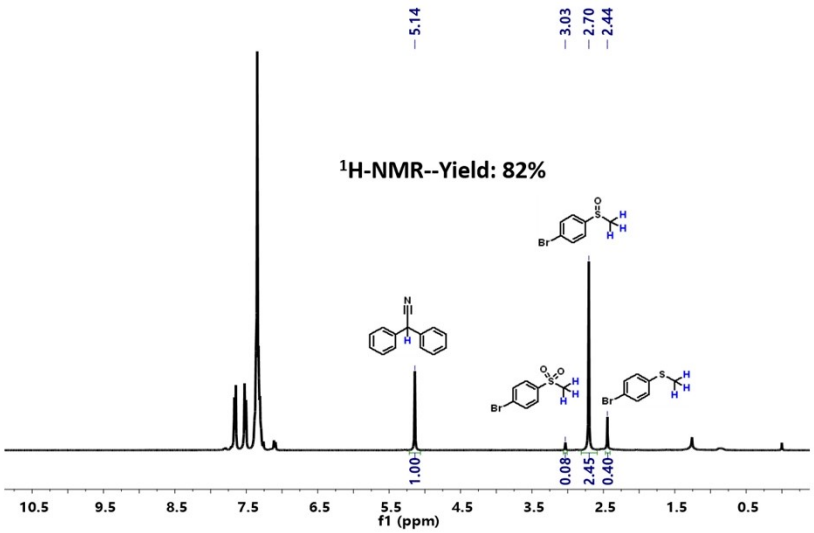

Fig. S31 Yield of **2d** catalyzed by **BT-COF1** and determined by ^{1}H-NMR with DPAT as internal standard.

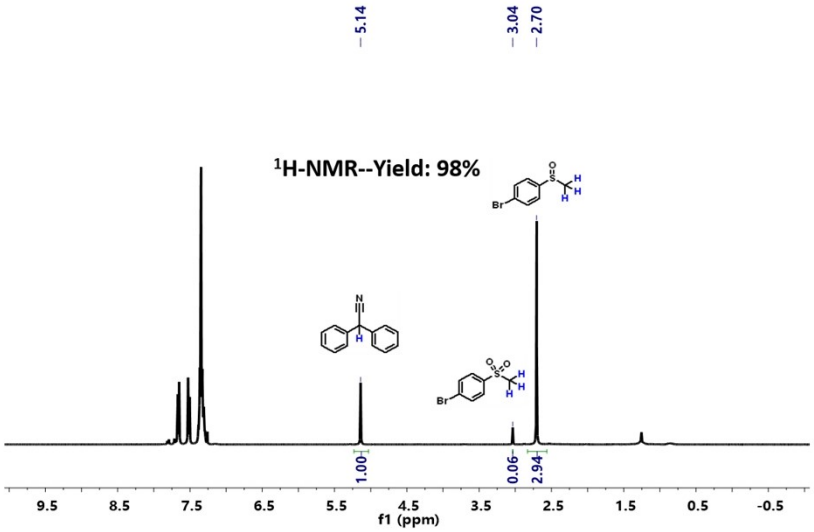

Fig. S32 Yield of **2d** catalyzed by **BT-COF2** and determined by ^{1}H-NMR with DPAT as internal standard.

Isolated 2d: ^{1}H-NMR ($CDCl_3$, 400 MHz): δ (ppm) 7.60-7.58 (d, J = 8.0 Hz, 2H), 7.46-7.44 (d, J = 8.0 Hz, 2H), 2.64 (s, 3H). ^{13}C-NMR ($CDCl_3$, 100 MHz): δ (ppm) 144.89, 132.56, 125.43, 125.15, 44.00. HRMS (ESI) m/z $[M+Na]^+$ calcd for C_7H_8BrOS:240.9299 found:240.9294.

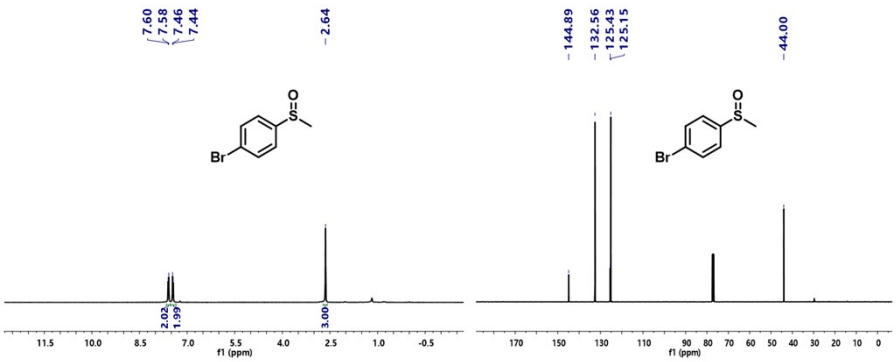

Fig. S33 ^{1}H-NMR (left) and ^{13}C-NMR (right) spectra of **2d**.

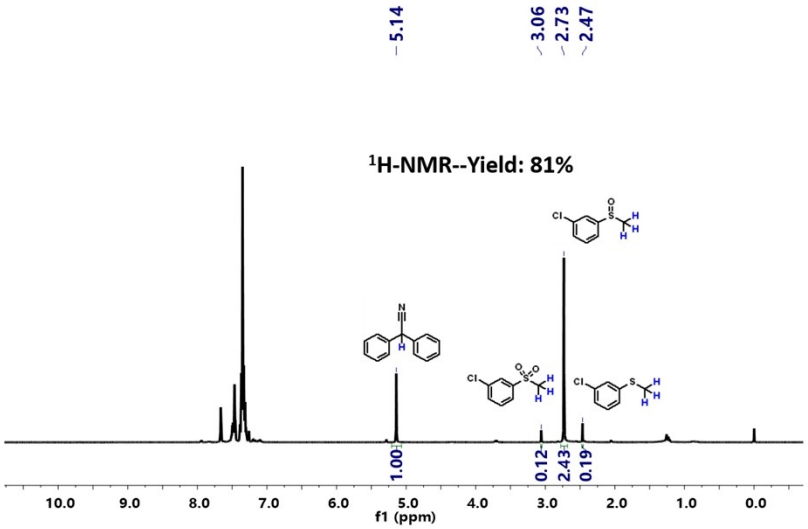

Fig. S34 Yield of **2e** catalyzed by **BT-COF1** and determined by ^{1}H-NMR with DPAT as internal standard.

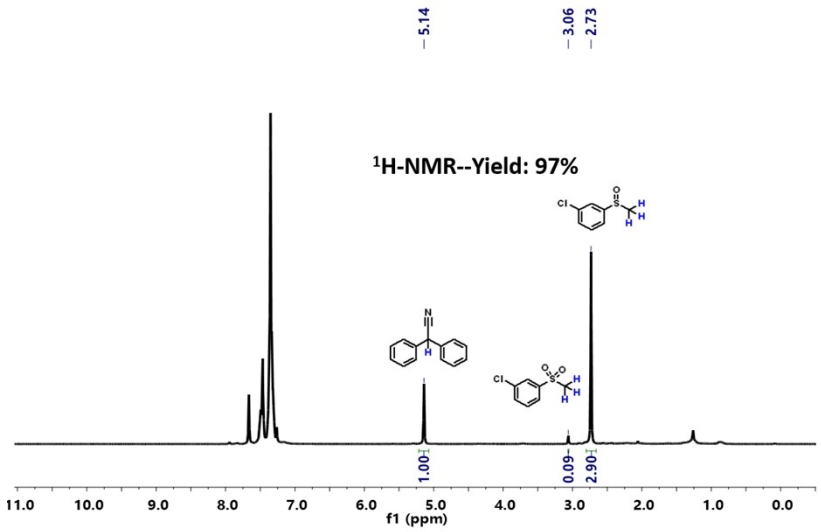

Fig. S35 Yield of **2e** catalyzed by **BT-COF2** and determined by ^{1}H-NMR with DPAT as internal standard.

Isolated 2e: ^{1}H NMR ($CDCl_3$, 400 MHz): δ (ppm) 7.63 (s, 1H), 7.46-7.42 (m, J = 16.0 Hz, 3H), 2.70 (s, 3H). ^{13}C-NMR ($CDCl_3$, 100 MHz): δ (ppm) 147.83, 131.17, 130.59, 123.60, 121.61, 44.01. HRMS (ESI) m/z $[M+Na]^+$ calcd for C_7H_8ClOS 196.9804 found:196.9783.

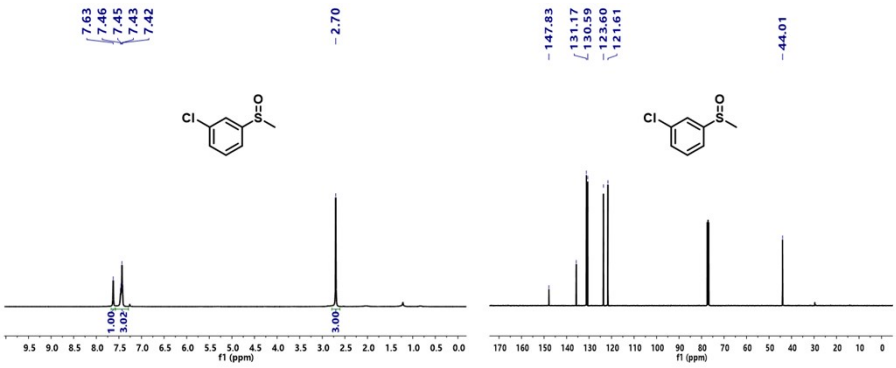

Fig. S36 ^{1}H-NMR (left) and ^{13}C-NMR (right) spectra of **2e**.

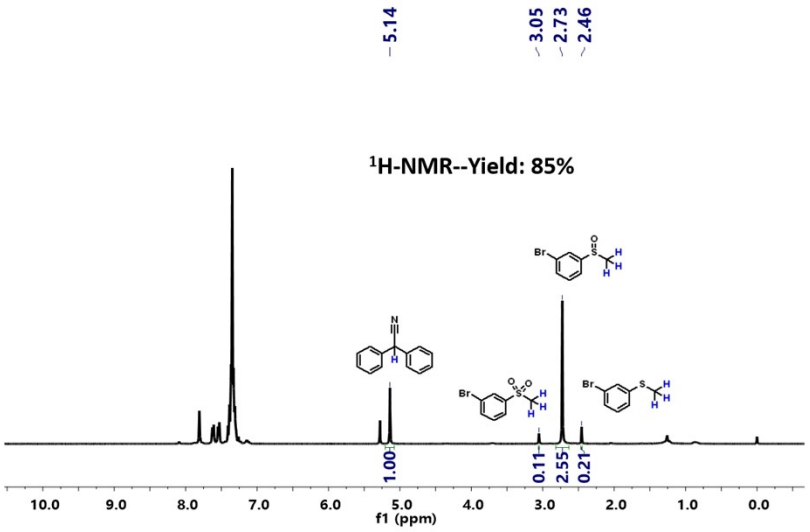

Fig. S37 Yield of **2f** catalyzed by **BT-COF1** and determined by ^{1}H-NMR with DPAT as internal standard.

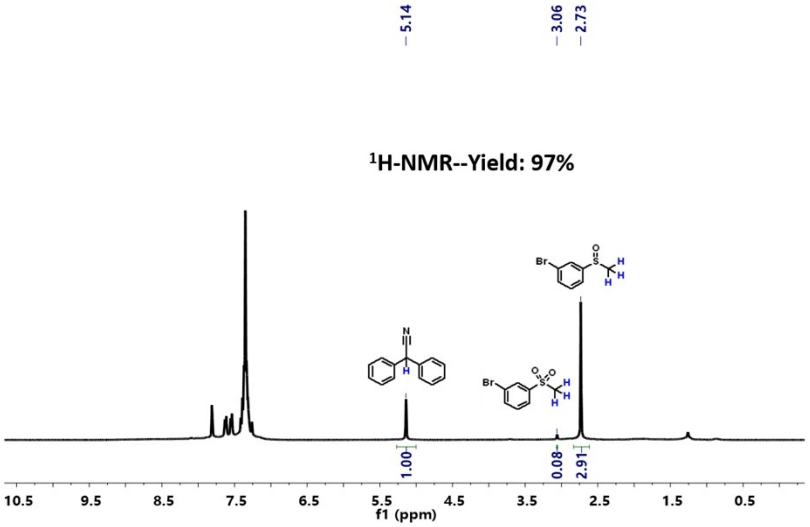

Fig. S38 Yield of **2f** catalyzed by **BT-COF2** and determined by ^{1}H-NMR with DPAT as internal standard.

Isolated 2f: ^{1}H-NMR ($CDCl_3$, 400 MHz): δ (ppm) 7.77 (s, 1H), 7.59-7.57 (d, J = 8.0 Hz, 1H), 7.51-7.49 (d, J = 8.0 Hz,1H), 7.38-7.34 (t, J = 16.0 Hz, 1H), 2.70 (s,3H). ^{13}C-NMR ($CDCl_3$, 100 MHz): δ (ppm) 147.98, 134.10, 130.85, 126.45, 123.58, 122.10, 44.04. HRMS (ESI) m/z $[M+Na]^+$ calcd for C_7H_8BrOS:240.9299 found:240.9305.

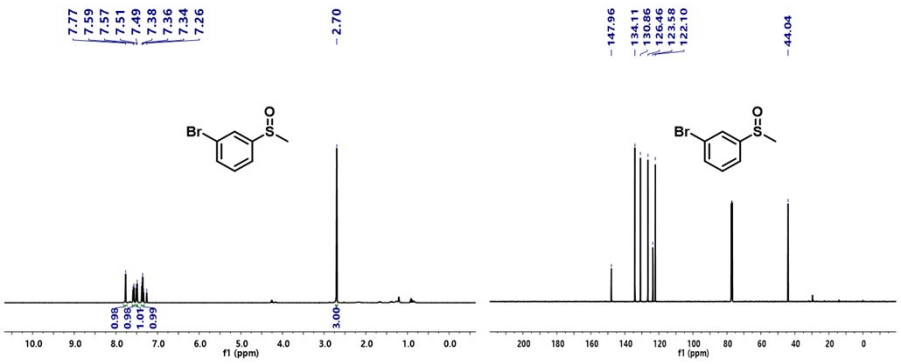

Fig. S39 ^{1}H-NMR (left) and ^{13}C-NMR (right) spectra of **2f**.

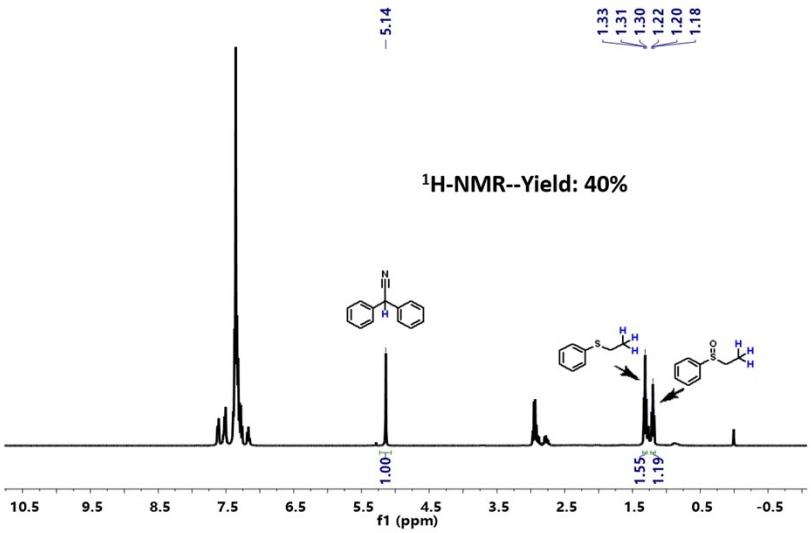

Fig. S40 Yield of **2g** catalyzed by **BT-COF1** and determined by ^{1}H-NMR with DPAT as internal standard.

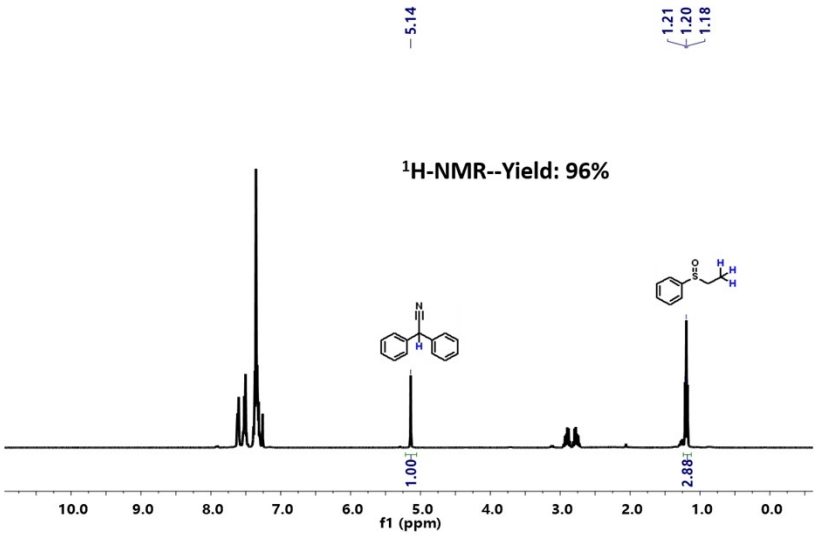

Fig. S41 Yield of **2g** catalyzed by **BT-COF2** and determined by ^{1}H-NMR with DPAT as internal standard.

Isolated 2g: ^{1}H-NMR ($CDCl_3$, 400 MHz): δ (ppm) 7.61-7.58 (m, *J* = 12.0 Hz, 2H), 7.53-7.47 (m, *J* = 24.0 Hz, 3H), 2.91-2.72 (m, *J* = 36.0 Hz, 2H), 1.20-1.16 (t, *J* = 16.0 Hz, 3H). ^{13}C- NMR ($CDCl_3$, 100 MHz): δ (ppm) 143.29, 130.92, 129.13, 124.16, 50.27, 5.94. HRMS (ESI) m/z $[M+Na]^+$ calcd for $C_8H_{10}OS$:177.0348 found:177.0346.

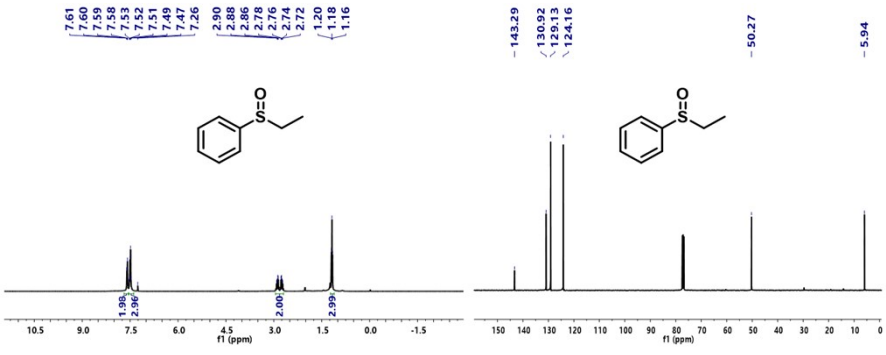

Fig. S42 ^{1}H-NMR (left) and ^{13}C-NMR (right) spectra of **2g**.

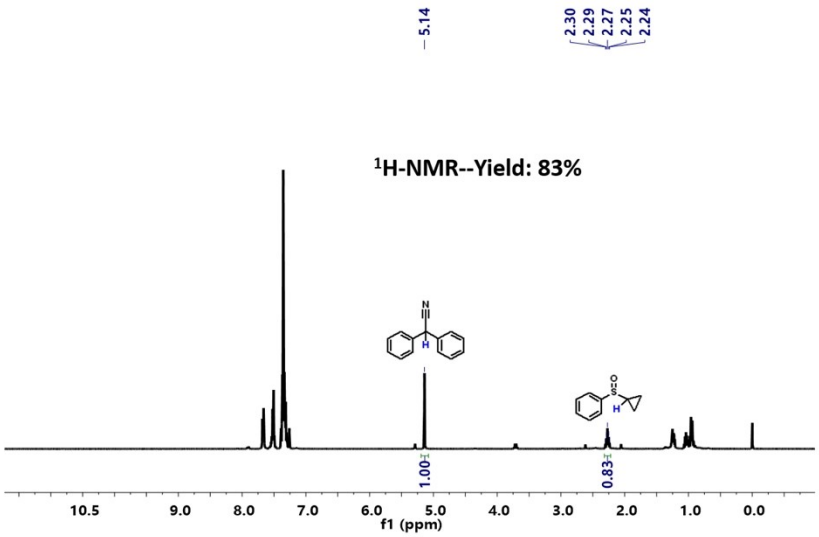

Fig. S43 Yield of **2h** catalyzed by **BT-COF1** and determined by ^{1}H-NMR with DPAT as internal standard.

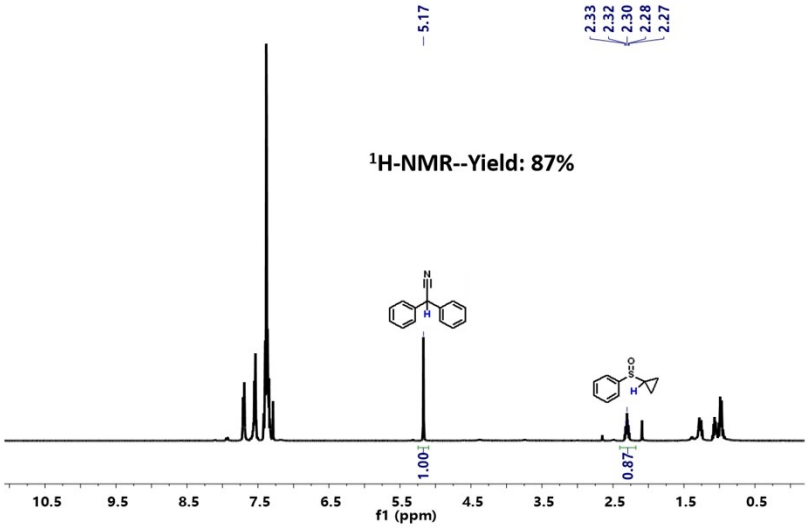

Fig. S44 Yield of **2h** catalyzed by **BT-COF2** and determined by ^{1}H-NMR with DPAT as internal standard.

Isolated 2h: ^{1}H-NMR ($CDCl_3$, 400 MHz): δ (ppm) 7.64-7.62 (m, *J* = 8.0 Hz, 2H), 7.48-7.46 (m, *J* = 8.0 Hz, 3H), 2.26-2.19 (m, *J* = 28.0 Hz, 1H), 1.21-1.17 (m, *J* = 16.0Hz, 1H), 1.00-0.89 (m, *J* = 44.0 Hz, 3H). ^{13}C-NMR ($CDCl_3$, 100 MHz): δ (ppm) 144.88, 130.92, 129.16, 124.01, 33.78, 3.41, 2.75. HRMS (ESI) m/z $[M+Na]^+$ calcd for $C_9H_{10}OS$:189.0350 found:189.0358.

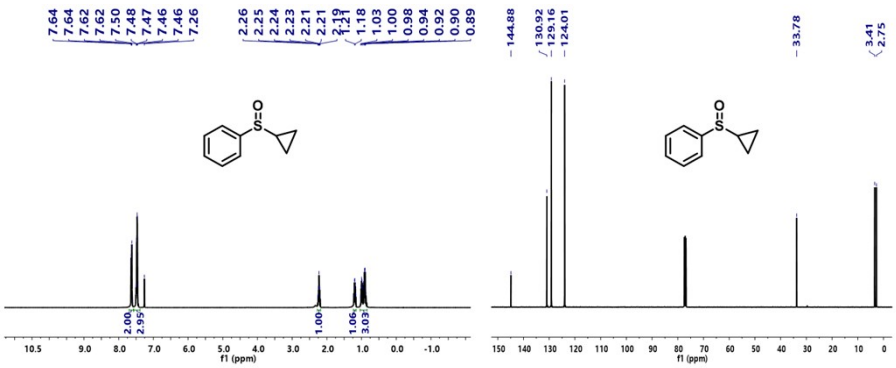

Fig. S45 ^{1}H-NMR (left) and ^{13}C-NMR (right) spectra of **2h**.

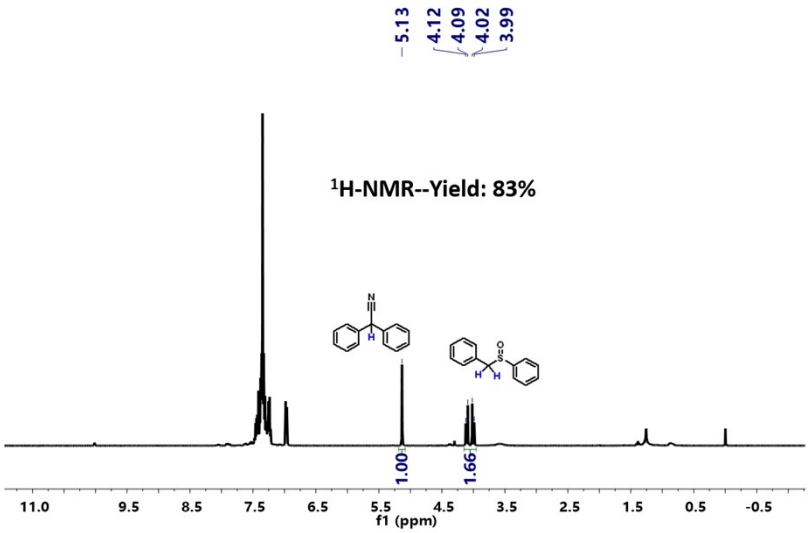

Fig. S46 Yield of 2**i** catalyzed by **BT-COF1** and determined by ^{1}H-NMR with DPAT as internal standard.

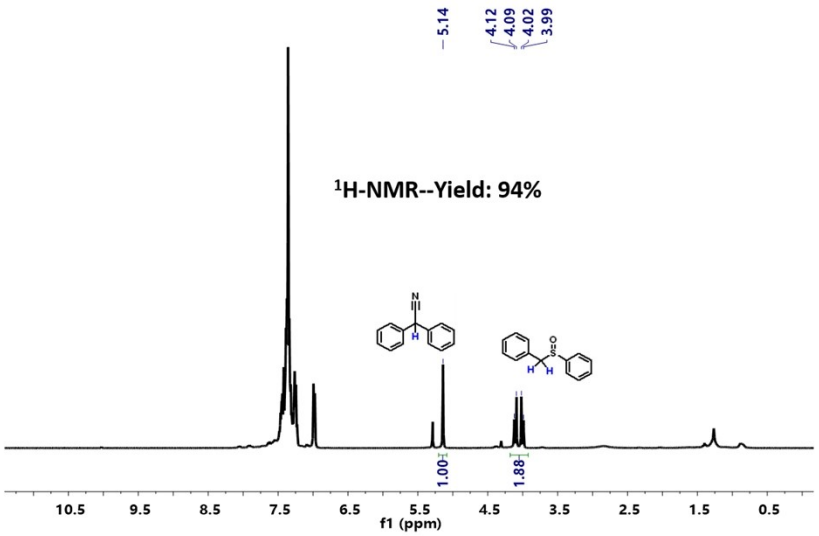

Fig. S47 Yield of 2**i** catalyzed by **BT-COF2** and determined by ^{1}H-NMR with DPAT as internal standard.

Isolated 2i: ^{1}H-NMR ($CDCl_3$, 400 MHz): δ (ppm) 7.49-7.37 (m, *J* = 48.0 Hz, 5H), 7.29-7.23 (m, *J* = 24.0 Hz, 3H), 7.00-6.98 (m, *J* = 8.0 Hz, 2H), 4.12-4.09 (d, *J* = 12.0 Hz, 1H), 4.02-3.99 (d, *J* = 12.0 Hz, 1H). ^{13}C-NMR ($CDCl_3$, 100 MHz): δ (ppm) 142.81, 131.17, 130.37, 129.16, 128.86, 128.46, 128.26, 124.46, 63.62. HRMS (ESI) m/z $[M+Na]^+$ calcd for $C_{13}H_{12}OS$:239.0507 found:239.0495.

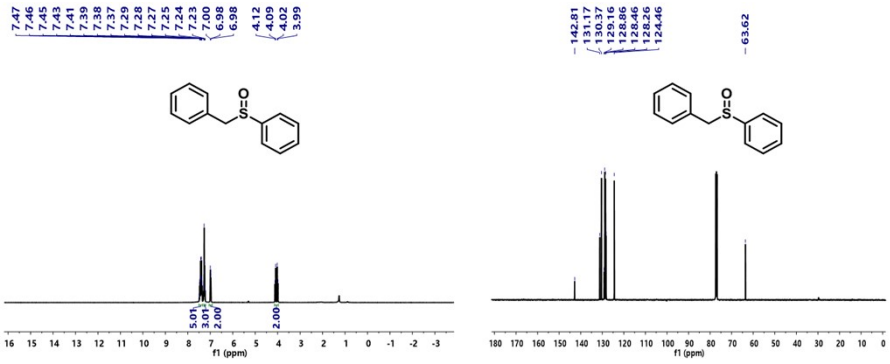

Fig. S48 ^{1}H-NMR (left) and ^{13}C-NMR (right) spectra of **2i**.

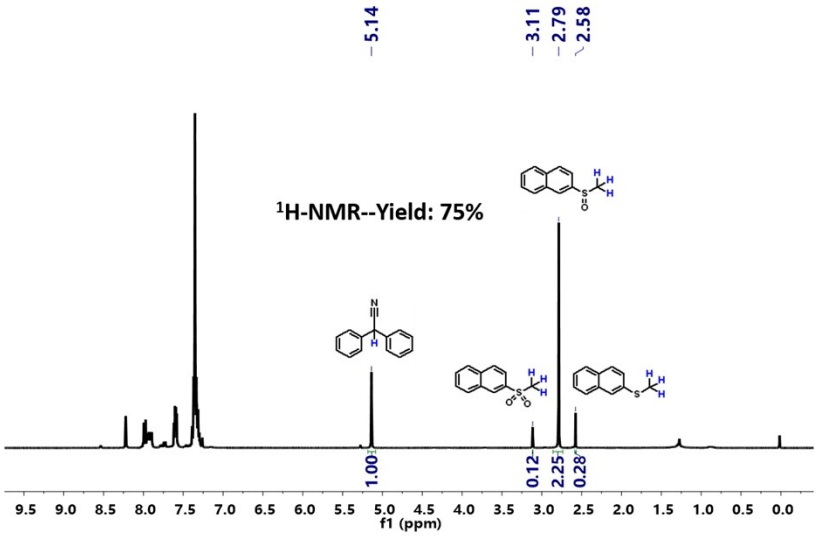

Fig. S49 Yield of **2j** catalyzed by **BT-COF1** and determined by ^{1}H-NMR with DPAT as internal standard.

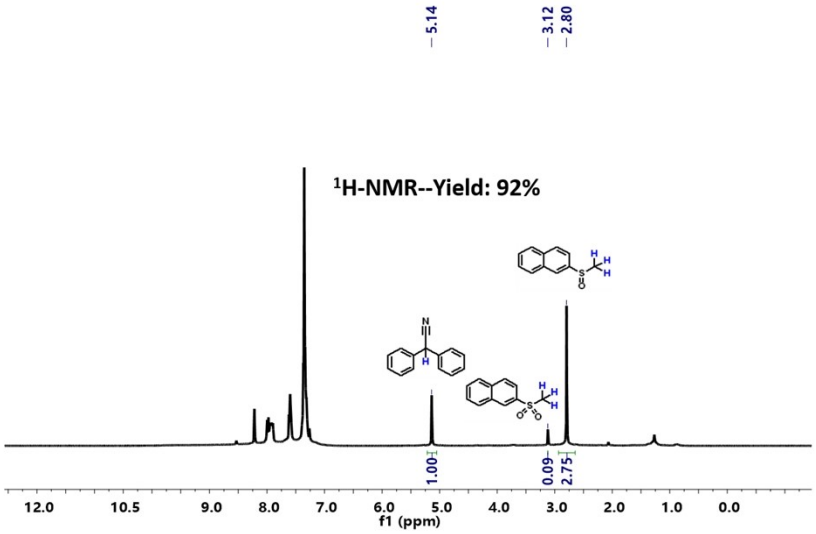

Fig. S50 Yield of **2j** catalyzed by **BT-COF2** and determined by ^{1}H-NMR with DPAT as internal standard.

Isolated 2j: ^{1}H-NMR ($CDCl_3$, 400 MHz): δ (ppm) 8.19 (s, 1H), 7.96-7.86 (m, *J* = 40.0 Hz, 3H), 7.58-7.54 (m, *J* = 16.0 Hz, 3H), 2.76 (s, 3H). ^{13}C-NMR ($CDCl_3$, 100 MHz): δ (ppm) 142.77, 134.42, 132.91, 129.62, 128.52, 128.08, 127.80, 127.37, 124.04, 119.46, 43.81. HRMS (ESI) m/z $[M+Na]^+$ calcd for $C_{11}H_{10}OS$:213.0350 found:213.0339.

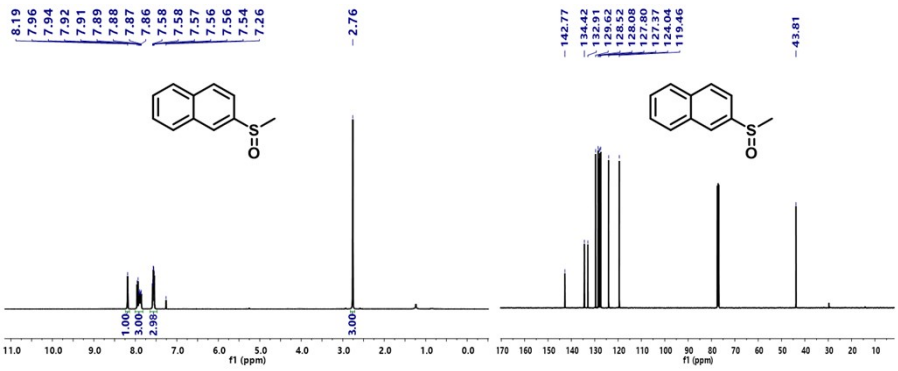

Fig. S51 ^{1}H-NMR (left) and ^{13}C-NMR (right) spectra of **2j**.

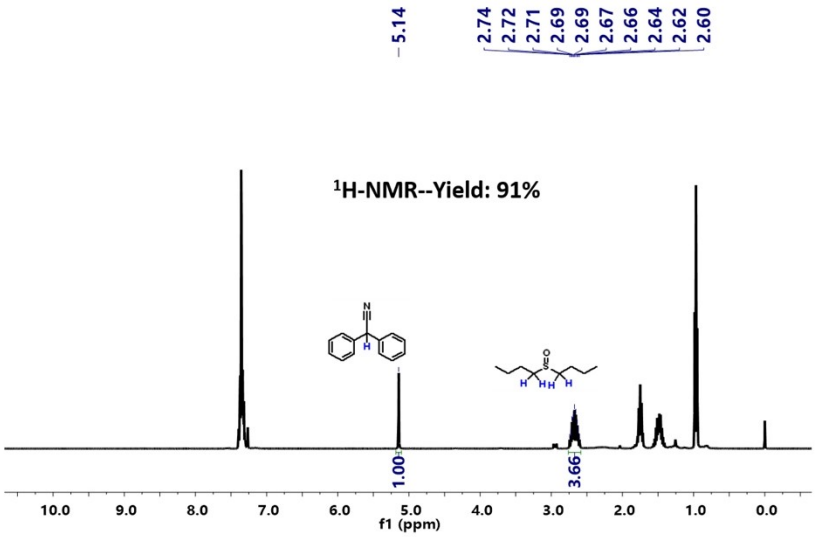

Fig. S52 Yield of **2k** catalyzed by **BT-COF1** and determined by ^{1}H-NMR with DPAT as internal standard.

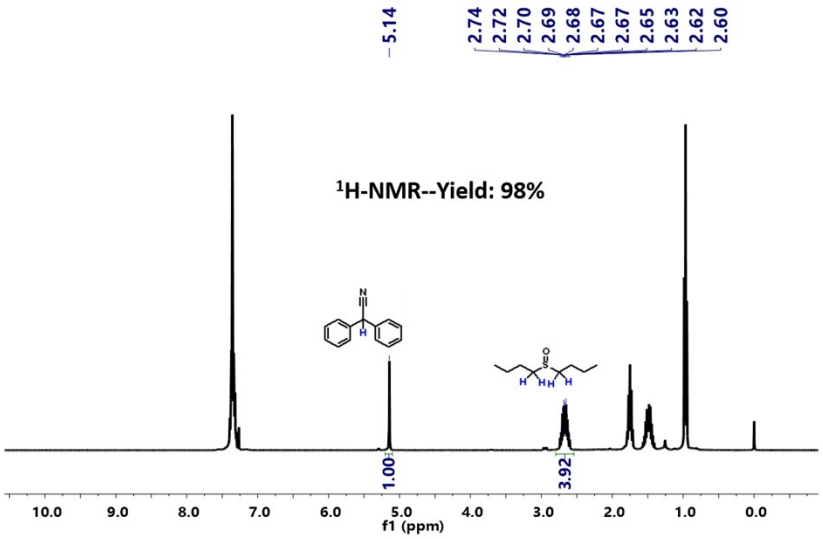

Fig. S53 Yield of **2k** catalyzed by **BT-COF2** and determined by ^{1}H-NMR with DPAT as internal standard.

Isolated 2k: ^{1}H-NMR ($CDCl_3$, 400 MHz): δ (ppm) 2.68-2.55 (m, *J* = 28.0 Hz, 4H), 1.74-1.67 (m, *J* = 28.0 Hz, 4H), 1.46-1.36 (m, *J* = 40.0 Hz, 4H), 0.94-0.90 (t, *J* = 12.0 Hz, 6H). ^{13}C- NMR ($CDCl_3$, 100 MHz): δ (ppm) 52.14, 24.59, 22.06, 13.65. HRMS (ESI) m/z $[M+Na]^+$ calcd for $C_8H_{18}OS$:185.0976 found:185.0977.

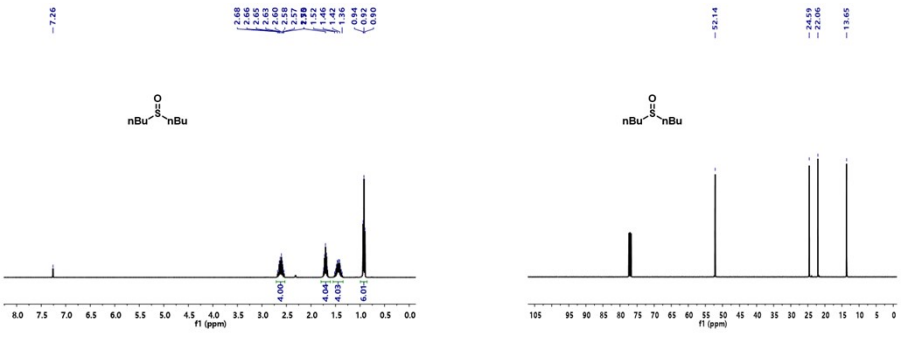

Fig. S54 ^{1}H-NMR (left) and ^{13}C-NMR (right) spectra of **2k**.

6.5. Recycling experiments

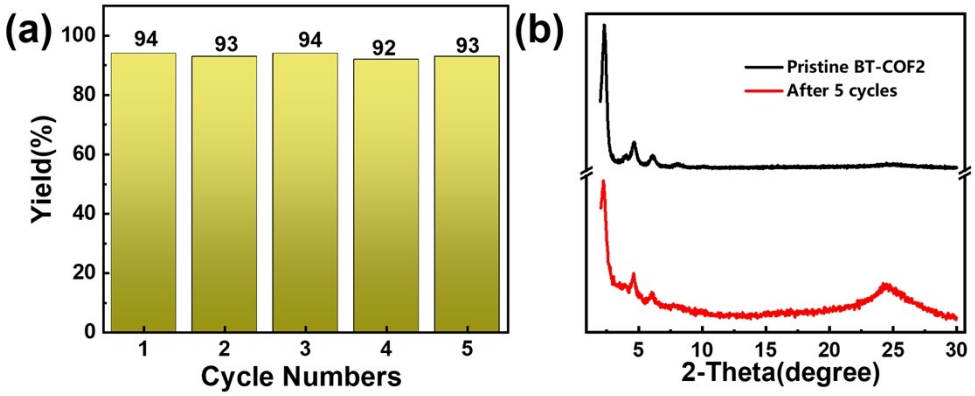

Fig. S55 (a) Recycling experiments. (b) PXRD spectra of photocatalyst **BT-COF2 (**before and after five cycles).

7. Sunlight irradiation

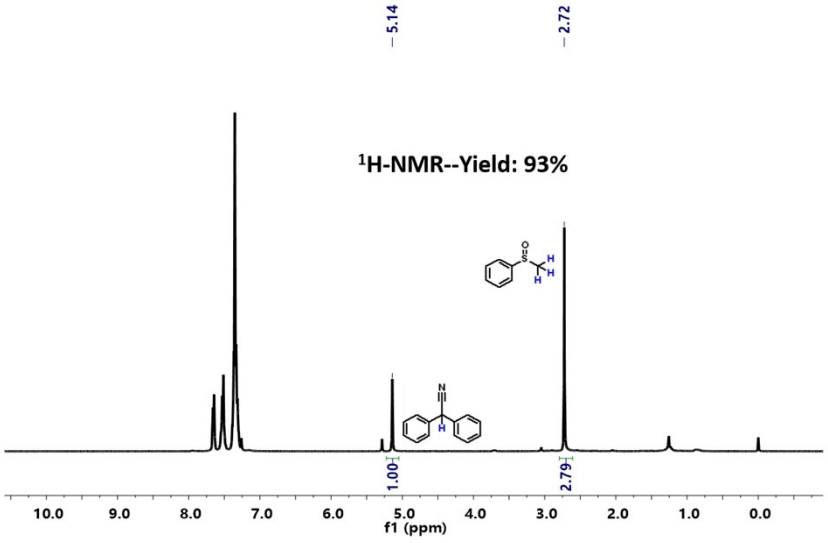

Fig. S56 Yield of 2**a** catalyzed by **BT-COF2** with the irradiation of natural sunlight and determined by ^{1}H-NMR with DPAT as internal standard.

8. Photocurrent curves

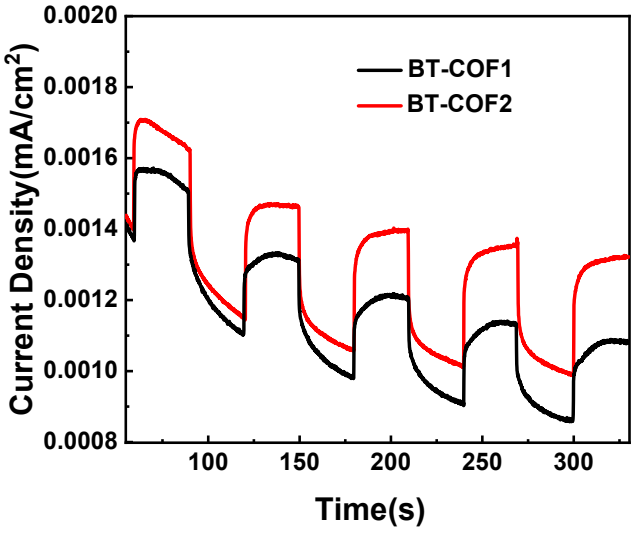

Fig. S57 Photocurrent responses of **BT-COF1** (black) and **BT-COF2** (red).

9. DFT calculations

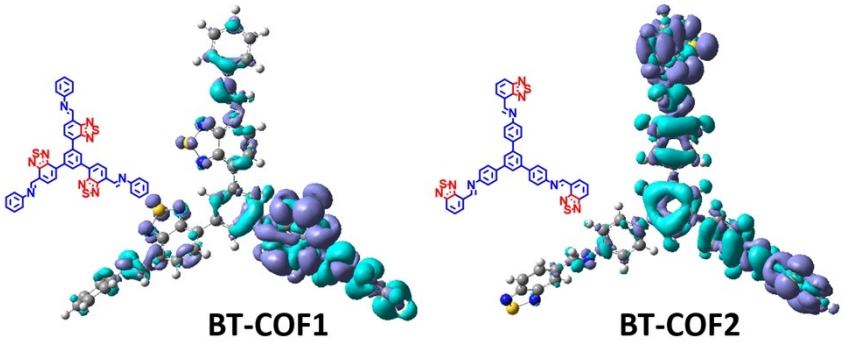

Fig. S58 Charge density difference between the ground and first singlet state based on the ground state structure, where the purple and blue colors represent an increase and decrease in electron density, respectively.

10. ESR spectrum

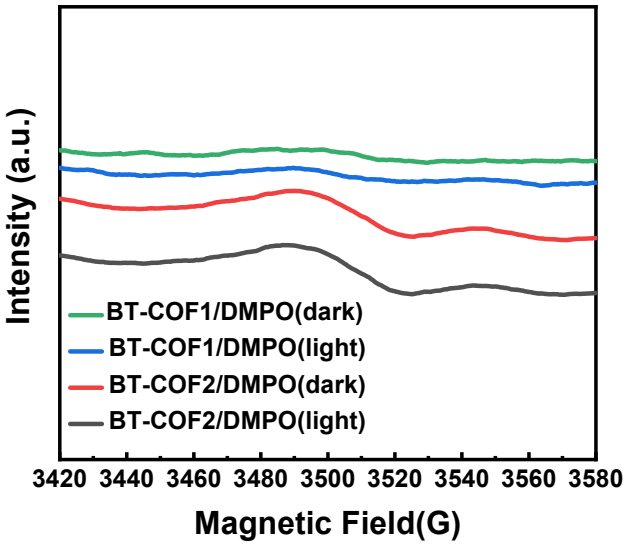

Fig. S59 ESR spectra of a mixture of COF (4 mg/mL) and DMPO (0.1M) in O_2-saturated EtOH in dark and upon light irradiation.

11. Crystallographic parameters

BT-COF1 Space group: *P3* a = 44.86 Å, b = 44.86 Å, c = 3.59 Å α = 90°, β = 90°, γ = 120°			
Atom	x	y	z
C1	0.298	-0.34658	0.0265
C2	0.3108	-0.36931	0.033
C3	0.28725	-0.40743	0.044
C4	0.25326	-0.42314	0.18636
C5	0.23234	-0.45809	0.18848
C6	0.24369	-0.47998	0.05743
C7	0.27723	-0.46533	-0.08404
C8	0.29856	-0.42969	-0.09344
C9	0.22092	-0.51735	0.06233
N10	0.23096	-0.53717	-0.08549
C11	0.21162	-0.57393	-0.10422
C12	0.17677	-0.59299	########
C13	0.15948	-0.62875	-0.01418
C14	0.17645	-0.64617	-0.13411
C15	0.21105	-0.62695	-0.24649

C16	0.2284	-0.59111	-0.2318
C17	0.15833	-0.6842	-0.13212
C18	0.12354	-0.70348	-0.2363
C19	0.10622	-0.73935	-0.21976
C20	0.12311	-0.75674	-0.09926
C21	0.15821	-0.73741	-0.00177
C22	0.17548	-0.70157	-0.01698
N23	0.10382	-0.7937	-0.08495
C24	0.11394	-0.81396	0.0543
C25	0.09117	-0.85172	0.04482
C26	0.05733	-0.86679	-0.09098
C27	0.03602	-0.9027	-0.10397
C28	0.04696	-0.92511	0.04101
C29	0.0811	-0.90891	0.18268
C30	0.10276	-0.87376	0.17103
C31	0.02288	-0.96373	0.03649
C32	0.03547	-0.98689	0.03212
N33	0.23757	0.59301	1.33166
S34	0.19617	0.56541	1.44928
N35	0.20061	0.53166	1.31798
N36	0.09628	0.07505	1.34584
S37	0.13759	0.10278	1.4682
N38	0.13381	0.13667	1.32253
H39	0.27086	-0.35673	0.00936
H40	0.28692	-0.48126	-0.19653
H41	0.32333	-0.42032	-0.22409
H42	0.19617	-0.52757	0.19582
H43	0.1626	-0.58083	0.09363
H44	0.13301	-0.64276	0.07917
H45	0.22461	-0.6396	-0.34854
H46	0.25506	-0.57662	-0.31918
H47	0.10987	-0.69079	-0.33421
H48	0.07943	-0.75375	-0.30237
H49	0.17261	-0.7495	0.08695
H50	0.20217	-0.68735	0.06978
H51	0.13896	-0.80362	0.18208
H52	0.04731	-0.85082	-0.19363
H53	0.01122	-0.9124	-0.2353
H54	0.0627	-0.9769	0.02154

BT-COF2 Space group: *P3* a = 44.20 Å, b = 44.20 Å, c = 3.59 Å

$\alpha = 90°, \beta = 90°, \gamma = 120°$			
Atom	x	y	z
C1	0.29699	-0.34991	-0.21146
C2	0.31312	-0.37045	-0.20836
C3	0.29293	-0.40759	-0.19292
C4	0.25786	-0.42593	-0.31885
C5	0.23801	-0.46221	-0.29234
C6	0.25258	-0.48137	-0.14645
C7	0.28735	-0.46377	-0.02572
C8	0.30708	-0.42753	-0.04513
C9	0.2311	-0.51953	-0.11624
N10	0.24425	-0.5376	0.02081
C11	0.22642	-0.57473	0.07249
C12	0.19047	-0.59642	3.26E-03
C13	0.17473	-0.63259	0.04944
C14	0.19408	-0.64811	0.17416
C15	0.22973	-0.62571	0.24869
C16	0.24517	-0.59042	0.19827
C17	0.17716	-0.68664	0.20745
C18	0.14235	-0.70713	0.32767
C19	0.12555	-0.74265	0.31685
C20	0.14177	-0.76059	0.18624
C21	0.17717	-0.74112	0.08226
C22	0.19453	-0.70445	0.08873
N23	0.12091	-0.79753	0.13998
C24	0.12924	-0.81813	-0.03012
C25	0.10276	-0.85517	-0.07159
C26	0.06848	-0.86759	0.05437
C27	0.04361	-0.90273	0.02153
C28	0.05197	-0.92631	-0.14821
C29	0.08625	-0.91342	-0.28309
C30	0.11146	-0.8783	-0.24026
C31	0.0253	-0.96411	-0.17533
C32	0.03542	-0.98952	-0.17861
N33	0.25212	0.36446	1.37403
S34	0.29293	0.39899	1.42591
N35	0.27937	0.42671	1.28056
H36	0.26898	-0.36266	-0.2126
H37	0.24567	-0.41294	-0.45407
H38	0.21129	-0.47541	-0.39174
H39	0.2991	-0.47792	0.09451
H40	0.33278	-0.4156	0.07809
H41	0.20439	-0.53179	-0.21151
H42	0.17413	-0.58625	-0.08948

H43	0.14745	-0.6482	-0.02169
H44	0.19133	-0.75365	-0.01408
H45	0.22098	-0.6903	-0.0162
H46	0.15461	-0.80848	-0.15677
H47	0.06094	-0.85035	0.18686
H48	0.01826	-0.91124	0.14353
H49	0.09365	-0.93006	-0.43004
H50	0.13759	-0.86905	-0.34596
H51	0.06281	-0.98138	-0.17629
N52	0.12174	0.30498	1.4513
S53	0.08097	0.27229	1.55141
N54	0.09207	0.24222	1.42671